

See discussions, stats, and author profiles for this publication at: <https://www.researchgate.net/publication/47427603>

Two-Dimensional Differential in Gel Electrophoresis (2D-DIGE) Analysis of Grape Berry Proteome during Postharvest Withering

ARTICLE in JOURNAL OF PROTEOME RESEARCH · OCTOBER 2010

Impact Factor: 4.25 · DOI: 10.1021/pr1005313 · Source: PubMed

CITATIONS

27

READS

122

7 AUTHORS, INCLUDING:



Mario Pezzotti

University of Verona

121 PUBLICATIONS 4,200 CITATIONS

SEE PROFILE



Kathryn Lilley

University of Cambridge

217 PUBLICATIONS 9,760 CITATIONS

SEE PROFILE



Eugenio Benvenuto

ENEA

67 PUBLICATIONS 1,793 CITATIONS

SEE PROFILE



Angiola Desiderio

ENEA

23 PUBLICATIONS 824 CITATIONS

SEE PROFILE

Two-Dimensional Differential in Gel Electrophoresis (2D-DIGE) Analysis of Grape Berry Proteome during Postharvest Withering

Mariasole Di Carli,^{*,†} Anita Zamboni,[‡] Mario Enrico Pè,[§] Mario Pezzotti,[‡] Kathryn S. Lilley,^{||} Eugenio Benvenuto,[†] and Angiola Desiderio^{*,†}

Laboratorio Biotecnologie, UT BIORAD-FARM, ENEA Casaccia, Rome, Italy, Department of Biotechnology, University of Verona, Verona, Italy, Scuola Superiore Sant'Anna, Pisa, Italy, and Cambridge Centre for Proteomics, Department of Biochemistry, Cambridge University, Cambridge, U.K.

Received May 28, 2010

The practice of postharvest withering is commonly used to correct quality traits and sugar concentration of high quality wines. To date, changes in the metabolome during the berry maturation process have been well documented; however, the biological events which occur at the protein level have yet to be fully investigated. To gain insight into the postharvest withering process, we studied the protein expression profiles of grape (*Corvina* variety) berry development focusing on withering utilizing a two-dimensional differential in gel electrophoresis (2D-DIGE) proteomics approach. Comparative analysis revealed changes in the abundance of numerous soluble proteins during the maturation and withering processes. On a total of 870 detected spots, 90 proteins were differentially expressed during berry ripening/withering and 72 were identified by MS/MS analysis. The majority of these proteins were related to stress and defense activity (30%), energy and primary metabolism (25%), cytoskeleton remodelling (7%), and secondary metabolism (5%). Moreover, this study demonstrates an active modulation of metabolic pathways throughout the slow dehydration process, including de novo protein synthesis in response to the stress condition and further evolution of physiological processes originated during ripening. These data represent an important insight into the withering process in terms of both *Vitis* germplasm characterization and knowledge which can assist quality improvement.

Keywords: *Vitis vinifera* • berry proteome • 2D-DIGE • plant protein extraction • withering

1. Introduction

Oenology technologies are mostly focused to enhance the aroma and structure of the wine product. The synthesis of secondary metabolites during ripening, which strongly contribute to aroma, taste, and color, have been widely studied.^{1,2} Although the accumulation of these secondary metabolites is highly dependent on the cultivar genotype, environmental conditions and agricultural practices are well-known to influence their abundance within grape berries.³ Postharvest dehydration is the typical methodology used to promote wines with special aroma, such as “Recioto” and “Amarone”. The techniques employed to bring about withering and as well as the terroir are major factors affecting the international success of both of these types of wines which are typically produced in Valpolicella area (Verona, Italy). In the case of Amarone, an

extremely robust dry tasting wine, the quality of the grape skin is a primary concern as this tissue contributes tannins, color, and intensity of flavor to the wine. The process of desiccation not only concentrates the juices within the grape but allows the further metabolization of the acids within the grape and promotes the polymerization of the tannins in the skin, which contributes to the overall balance of the final product. The “Recioto della Valpolicella” wine is produced when the fermentation is stopped early, resulting in wine which contains residual sugar, characterized by a sweeter taste. Thus, quality and reproducibility of successive vintages are highly dependent on knowledge of the sugar content of the desiccating berries. The postharvesting procedure, which can be prolonged up to three months, essentially exploits the dehydration process to increase sugar content and volatile compounds.^{4,5} High temperature and concurrent high ventilation, which are essential within the postharvesting vinification technique, induce water evaporation in the grape berry despite the fact that it is covered in a thick wax layer.⁶ Significant metabolic changes in grape fruits have been observed as a consequence of water loss.⁷ During postharvest drying, a biphasic pattern of total protein accumulation, associated with the gradual weight loss, was observed which was thought to be due primarily to de novo synthesis of proteins involved in stress response.⁶ A few studies have investigated the postharvest fruit adaptation to environ-

* To whom correspondence should be addressed: (A.D.) Laboratorio Biotecnologie, UT BIORAD-FARM, ENEA Casaccia Research Centre, via Anguillarese 301, 00123 Rome, Italy. E-mail: desiderio@enea.it. Tel: ++39 06 30484176. Fax: ++39 06 30484808; (M.D.) Laboratorio Biotecnologie, UT BIORAD-FARM, ENEA Casaccia Research Centre, via Anguillarese 301, 00123 Rome, Italy. E-mail: mariasole.dicarli@enea.it. Tel: ++39 06 30486890. Fax: ++39 06 30484808.

[†] Laboratorio Biotecnologie, UT BIORAD-FARM.

[‡] University of Verona.

[§] Cambridge University.

^{||} Scuola Superiore Sant'Anna.

mental stresses at a molecular level, analyzing the role of phospholipase D, stilbene synthase, and phenylalanine ammonia lyase genes within the withering process.^{8–10}

The recent progress with respect to the characterization and annotation of the grape genome provides an extraordinary tool for genome-wide analyses, enabling transcriptomics studies and supporting the interpretation of metabolomics and proteomics data.¹¹ The next critical challenge is to provide biological meaning to this huge amount of data by annotating genes and integrating them within their biological context.¹² Around half of the predicted genes are specific for grape and mostly implicated in traits influencing wine quality through secondary metabolites production and related to grape susceptibility to pathogens.¹³ Microarray platforms have been designed to give an overview of the gene activity in several physiological studies, including withering process.^{1,5,14,15}

Although sequencing of total cDNA (RNA-Seq technology) of grape berry demonstrated the dynamic modulation of plant transcriptome during ripening,¹⁶ different stimuli may exert their effect on berry development essentially at the translational and post-translational level. To date, no metabolomic and proteomic data are reported on dynamic changes occurring during withering. Moreover, despite the fact that proteins and peptides represent minor constituents of wine, they significantly contribute to the quality of the final product because they affect taste, clarity, and stability. In the last few years, although a limited number of studies have been published on the proteomic analysis of grape ripening,^{17–21} proteome modification during the withering phase remains completely unexplored. The aim of this work is to investigate changes in the proteome during berry withering, utilizing the two-dimensional differential in gel electrophoresis (2D-DIGE) quantitative proteomics technology to determine the protein dynamic changes during postharvesting in *Vitis vinifera* cv. *Corvina* berry, which is the base grape variety for Amarone and Recioto wines. We underlined how proteomic profile associated with the ripening process is modified after harvesting, affecting molecular composition of the berry before vinification.

In our analysis, we chose to consider grape berry as skin and pulp combined tissue (pericarp), which together contribute to final product characteristics. Grape skin is undoubtedly one of the main sources of aroma and color compounds. Aromas arise from volatile compounds, such as terpenes, norisoprenoids, and thiols, but sugars and proteins contribute as well to the organoleptic properties.²² Nevertheless, the contribution of the pulp is not negligible, as this tissue provides a high value nutritional content, mainly consisting of free amino acids and hexose sugars, which are transformed into alcohol during the fermentation process.⁷ Moreover, pulp represents the main source of many metabolites and polypeptides.²³

The contribution of the seeds to wine properties is also appreciable, affecting the content of total phenolics and free anthocyanins, as well as color intensity and a stabilization of wine color through time.^{24,25} Despite this evidence, seeds were excluded from our analysis as the high content of phenols and many other compounds which coprecipitate with proteins interfere with protein extraction.²⁶ Moreover, it was felt that the difficulty in predicting the exact contribution of the seed to the total tissue samples for each stage of maturation and withering would lead to high levels of variation that may obscure physiologically significant changes in protein abundance.

In summary, in this study, we evidenced how the protein profile associated with ripening process is modified after

harvesting, thus influencing the fluctuations in the berry molecular components before vinification.

2. Material and Methods

2.1. Plant Material. *Vitis vinifera* cv *Corvina* berries were sampled during the 2006 growing season in Valpolicella area (Verona, Italy) at three developmental time points and three additional time points during the three months postharvest withering process. The three developmental time points were 71, 98, and 112 days after fruit set, corresponding to veraison (sample V), early ripening (or postveraison, named sample PV), and late ripening (sample R). The sampled berry stages corresponded to the developmental stages E-L 35, E-L 36, and E-L 38, respectively, described by Coombe.²⁷ Basal bunches of grapes were collected from the middle part of the vine branch. At each time point, bunches were sampled from the same row of vines. To account for biological variance, berries were collected from different bunches and from different part of the bunch, deseeded, and pooled. After deseeding, berries were immediately frozen at -80°C prior to protein analysis. Post-harvest withering was analyzed by collecting berry clusters and storing them in a special room, at room temperature ($13\text{--}17^{\circ}\text{C}$ in the period of withering, from the half of October to December) and a controlled relative humidity not exceeding 65%. The three withering time points (samples WI, WII, and WIII) were 35, 56, and 91 days after harvest. Three or four independent protein extractions were carried out for each stage. This resulted in 22 biological replicates that were analyzed by two-dimensional gel electrophoresis (2-DE) coupled to difference in gel electrophoresis (DIGE) technology (the experimental design is supplied as Supporting Information, Table S1). A pool of deseeded berries, corresponding to approximately 5 g, was used for each sample extraction.

Mean Brix degree values were recorded at each sampling stage using a PR-32 bench refractometer (Atago Co.) to measure sugar concentration. Berry weight was determined by averaging the weight of 400 berries, and percentage weight loss in withering berries was calculated using mature berries (sample R) as a reference.

2.2. Protein Extraction. TCA-acetone extraction was adapted from the method described by Tsugita et al.,²⁸ with some modifications. Berry tissue (5 g) was ground to a fine powder in a mortar with liquid N_2 . The resulting powder was finely homogenized using Ultraturrax homogenizer in 20 mL of cold acetone and filtered by Miracloth paper (Amersham). After suspension in 20 mL of 10% TCA, 2% DTT in cold acetone containing protease inhibitor cocktail Complete (Roche), proteins were precipitated at -20°C overnight. The pellet collected after centrifugation at 8000g for 1 h at 4°C was then mixed with 0.07% DTT containing protease inhibitor cocktail in cold acetone and placed at -20°C for 1 h. Proteins were collected by centrifugation at 8000g for 1 h at 4°C , washed once with cold methanol, and then at least three times with cold acetone (until the supernatant was colorless) and air-dried under laminar flow.

Dry protein pellet obtained from TCA-acetone extraction was dissolved by shaking at room temperature for 1 h in solubilization buffer (8 M urea, 2% ASB-14, 10 mM Tris-HCl, pH 8.0, 5 mM magnesium acetate). The supernatant obtained after centrifugation at 14000g for 40 min was purified using Clean-Up kit (GE Healthcare) and used for one-dimensional gel electrophoresis (1-DE) and 2-DE. Protein concentration was

quantified using the DC Protein Assay (BioRad) and bovine serum albumin as a standard.

1-DE was carried out in 12% polyacrylamide gels using the BioRad Mini Protean II System. Protein samples were dissolved in 62 mM Tris-HCl, pH 6.8, 20% v/v glycerol, 1.8% w/v SDS, 175 mM β -mercaptoethanol, traces of bromophenol blue and heated at 100 °C for 5 min. Protein electrophoresis broad range markers from GE Healthcare were used. Gels were silver stained according to Oakley et al.²⁹

2.3. 2-DE. IPG-strips (pH 4–7/18 cm) containing solubilized protein samples were passively rehydrated overnight at room temperature with 350 μ L of isoelectrofocusing (IEF) buffer (7 M urea, 2 M thiourea, 13 mM DTT, 2% w/v ASB-14, 1% IPG buffer). The amount of protein loaded onto an IPG-strip (GE Healthcare) was 100 μ g and 600 μ g for analytical and preparative runs, respectively. IEF was performed on an IPGphor unit (GE Healthcare) at 20 °C, using a 50 μ A current limit per strip and a program setting of 3 h at 300 V, 1 h at 500 V, 6 h at 1000 V, 5 h at 8000 V (analytical gels) or a 60 μ A current limit per strip and a program setting of 10 h at 200 V, 3 h at 300 V, 1 h at 500 V, 6 h at 1000 V, 5 h at 8000 V (preparative gel). After focusing, proteins were reduced with 1% w/v DTT for 15 min and alkylated with 2.5% w/v iodoacetamide for 15 min, by independently incubating each strip in 10 mL of 50 mM Tris-HCl, pH 8.8, 6 M urea, 30% v/v glycerol, 2% w/v SDS, containing traces of bromophenol blue. Electrophoresis in the second dimension was carried out using the Ettan DALT twelve unit (GE Healthcare) and 12.5% polyacrylamide gels (18 cm \times 20 cm \times 1 mm) in 250 mM Tris-HCl, pH 8.3, 1.92 M glycine, 1% w/v SDS, at 15 °C, applying 2 W/gel for 30 min and 20 W/gel for further 4–5 h. Gels were silver stained according to Oakley et al.²⁹ (analytical gels) or Shevchenko et al.³⁰ (preparative gel).

2.4. 2D-DIGE. Before electrophoresis, protein samples were covalently labeled using the CyDyes DIGE Fluors (Cy2, Cy5, and Cy3, GE Healthcare) according to the manufacturer's instructions.³¹ Each dye (1 mM stock) was freshly diluted with anhydrous dimethylformamide and centrifuged at 12000g, at room temperature, for 5 min, just prior the labeling reaction. Each protein extract (50 μ g) was mixed with 200 pmol of amine-reactive cyanine dyes and incubated for 30 min in the dark.³² An aliquot of a pool of all biological samples compared in the experiment was labeled with Cy2 to provide a common internal standard across all gels in the experiment. The reactions were then quenched by adding 1 μ L of 10 mM lysine, which reacts with the remaining free NHS esters of the cyanine dyes, and incubating in the dark for 10 min. An equal volume of 7 M urea, 2 M thiourea, 130 mM DTT, 2% w/v ASB-14, 2% IPG buffer, was added and the samples were incubated for further 15 min in the dark. The final volume of each sample mixture was adjusted to 350 μ L with IEF rehydration buffer and 2-DE was performed on pH 4–7 strips (GE Healthcare), as described above. To avoid artifacts due to preferential labeling and to ensure statistical significance, a random design with a dye-swap approach was adopted. A total of 12 gels were run, 11 analytical gels representing 3–4 biological replicates according to the experimental design (Supporting Information, Table S1) and one preparative gel.

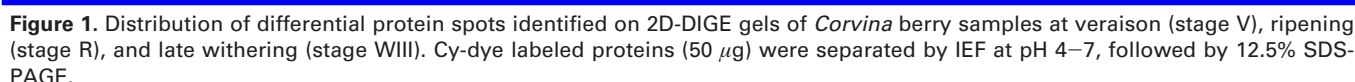
2.5. Gel Imaging and Statistical Analysis. After 2-DE, Cy-Dye-labeled proteins were visualized using the Typhoon 9410 Imager (GE Healthcare) set at the appropriate wavelengths for each dye. To ensure maximum pixel intensity for the three dyes (between 40 000 and 60 000 pixels), all gels were scanned at 100 μ m resolution and the photo multiplier tube (PMT) voltage

was set between 500–700 V. The scanned gel images were then transferred to the ImageQuant V5.2 software package (GE Healthcare). After cropping, the images were exported to the DeCyder Batch Processor and differential-in gel analysis (DIA) modules (GE Healthcare) for statistical analysis.

To compare protein spots across gels, a match set was created from the images of all 12 gels. The statistical analysis of protein level changes between different maturation stages was performed by the DeCyder-BVA (Biological Variation Analysis, v.6.5) module. The gel with the best resolution and the largest number of spots was chosen as the master gel. Landmark spots were manually defined to improve the automated matching results. Preparative cy-dye labeled gels were scanned and matched with the master gel in order to assign the right correspondence for spot picking.

Statistic analysis was performed taking into account both univariate and multivariate analysis using DeCyder software v.6.5 (GE Healthcare). An univariate analysis one way-ANOVA was performed using the DeCyder-BVA module and applying the false discovery rate (FDR) to minimize the number of false positives. A q -value of 0.05 was specified corresponding to the lowest FDR at which the protein is called significant. Data were normalized for computing the fold changes. Protein spots with a statistically significant variation ($p \leq 0.05$), showing a difference in volume over 1.5 fold compared to veraison sample, were selected as differentially expressed and analyzed by mass spectrometry. Multivariate analysis based on unsupervised nonhierarchical (k-means procedure), hierarchical clustering, and principle component analysis (PCA) was performed to assess global changes in ripening/withering responsive proteins. PCA allows for grouping of grape samples with overall similar expression characteristics and for identifying proteins, which are responsible for the differences between groups. Cluster analysis and visualizations were performed using the DeCyder-EDA (Extended Data Analysis) module.

2.6. Protein Digestion and LC-ESI-MS/MS Analysis. In gel reduction and alkylation was carried out using DTT and iodoacetamide, respectively. Digestion with trypsin was performed according to Coulthurst et al.³³ For LC-MS/MS experiments, an Eksigent NanoLC-1D Plus (Eksigent Technologies, Dublin, CA) HPLC system coupled to a LTQ Orbitrap mass spectrometer (ThermoFisher, Waltham, MA) was used. Separation of peptides was performed by reverse-phase chromatography employing a flow rate of 300 nL/min and an LC-Packings (Dionex, Sunnyvale, CA) PepMap 100 column (C18, 75 μ m i.d. \times 150 mm, 3 μ m particle size). Peptides were loaded onto a precolumn (Dionex Acclaim PepMap 100 C18, 5 μ m particle size, 100 Å, 300 μ m i.d. \times 5 mm) with 0.1% formic acid for 5 min at a flow rate of 10 μ L/min. After elution of peptides from the precolumn onto the analytical column, an elution gradient of 5–50% B in 50 min was employed where solvent A was 0.1% formic acid in water and solvent B was 0.1% formic acid in acetonitrile. The LC eluant was sprayed into the mass spectrometer by means of a New Objective nanospray source. All m/z values of eluting ions were measured in the Orbitrap mass analyzer, set at a resolution of 7500. Peptide ions with charge states of 2+ and 3+ were then isolated and fragmented in the LTQ linear ion trap by collision-induced dissociation and MS/MS spectra were acquired. Postrun, the data were processed using Bioworks Browser (version 3.3.1 SP1, ThermoFisher). Briefly, all MS/MS data were converted to *dta* (text) files using the Sequest Batch Search tool (within Bioworks). The *dta* files were converted to a single *mgf* file using a SSH script in the



RNA was isolated according to Rezaian and Krake³⁶ and quantified by spectrophotometry (ATI Unicam). An aliquot of each RNA sample was also analyzed using an Agilent 2100 Bioanalyzer. Total RNA (1 μ g) was amplified using the SuperScript Indirect RNA Amplification System (Invitrogen), to incorporate amino-allyl UTP (aRNA) and was fluorescently labeled with Alexa Fluor 647. The purified labeled aRNA was quantified by spectrophotometry as above. A 3- μ g sample of labeled RNA was hybridized to the array according to the manufacturer's recommendations (http://www.combimatrix.com/support_docs.htm). The array was scanned with a ScanArray 4000XL (Perkin-Elmer). TIFF images were exported to the Microarray Imager 5.8 (CombiMatrix) for densitometric analysis. A scale-normalization was applied to raw data.³⁷ Probe

3.1. Quantitative Proteome Analysis of *Corvina* Grape Berry. The dynamic proteomic profile of *Corvina* grape berry development was described by 2D-DIGE analysis from veraison to ripening and full postharvesting, providing the first exhaustive description of physiological changes occurring during the previnification process. Representative 2D-DIGE maps of proteins extracted using an optimized extraction procedure are provided as Supporting Information (Figure S1). Figure 1 shows the characteristic distribution of the most abundant proteins at the veraison stage, in mature and withered berries, indicating a specific activation of metabolic pathways according to the developmental and maturation time. An average of 870 protein spots were detected in each sampling stage. A complete list of analyzed protein spots is provided as Supporting Information (Table S2). The number of spots analyzed for each of the six stages did not change in a significant way from development to withering (Supporting Information, Figure S2). After normalization, protein spots were subjected to nonhierarchical clustering using the k-means procedure to assess for global changes in the ripening-withering responsive proteins compared to veraison. Six different clusters were created from all protein data sets on the basis of similar expression profiles

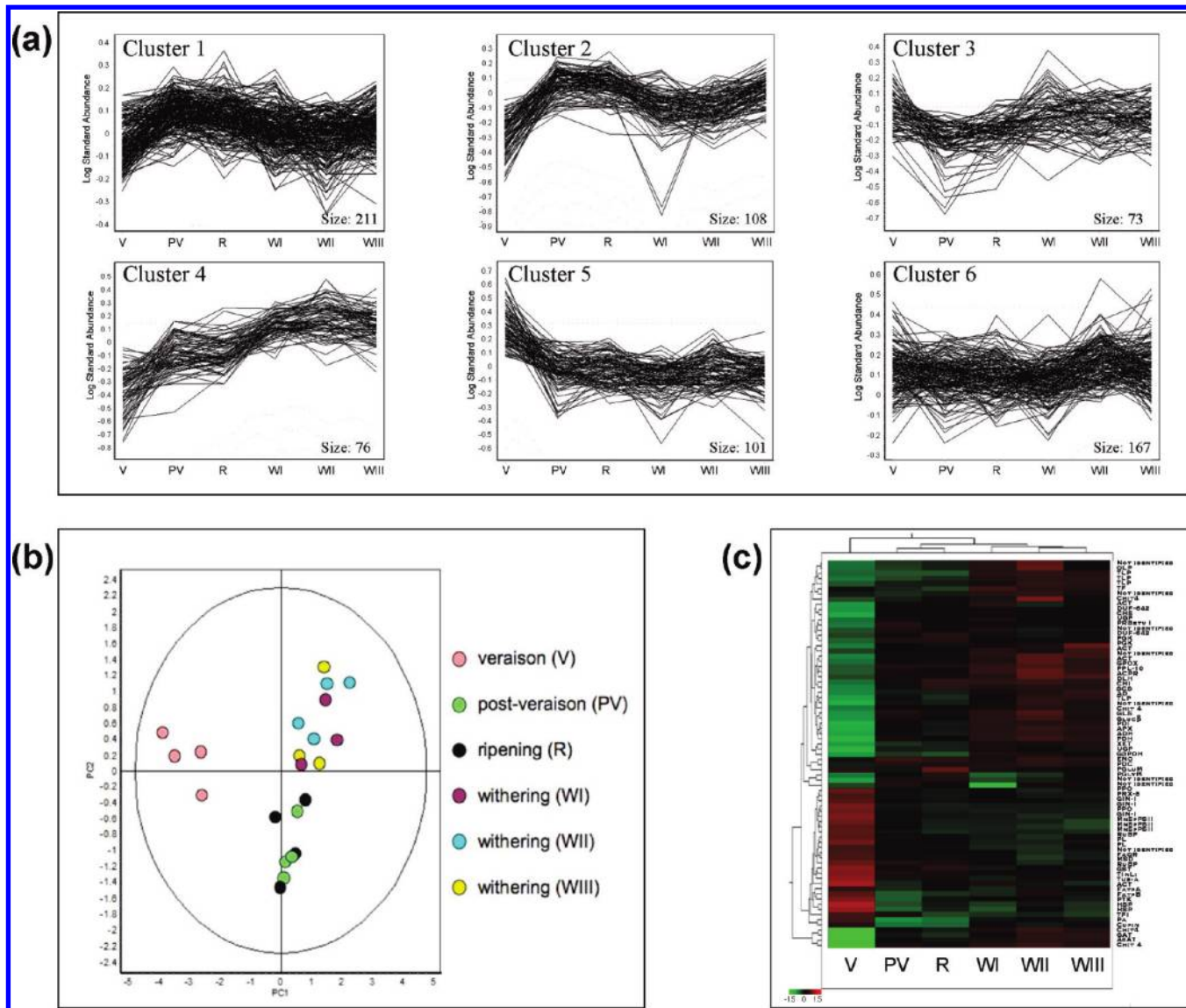


Figure 2. Multivariate analysis of *Corvina* berries sampled at six different stages: veraison (V), postveraison (PV), full ripening (R), and three withering stages (WI, WII, WIII) (a). Nonhierarchical analysis of proteins present in 80% of spot map according to k-means procedure (total 736 proteins). The 90 differential proteins whose abundance changed over development and withering are part of the protein set here analyzed. The number of proteins ascribed to each cluster is reported as "size". Cluster 1 and cluster 2 included spots abundant in the mature berries, whose intensity decreased at the beginning of the withering and slightly increased at the end of the withering phase. Cluster 3 contained spots with a higher intensity at the onset of the withering phase. Cluster 4 grouped protein spots that showed a gradual increasing volume during development, reaching their maximum concentration at the end of withering. Cluster 5 included spots whose intensity gradually decreased during the development process. Cluster 6 showed proteins with an invariable expression profile throughout all stages (b). PCA of the 90 spots that showed at least a 1.5-fold change in level compared to the veraison stage (ANOVA, $p \leq 0.05$); each dot represents the spot map of a single sample. Three or four biological replicates (represented with the same color) were visualized for each stage. The two principal components PC1 and PC2 resulted 61.9% and 14.1%, respectively (c). Two-way hierarchical clustering analysis of the 90 differential proteins (listed on the right) expression profiles according to ANOVA analysis. Red indicates proteins activation and green represents repression according to the color scale at the bottom of the figure.

(Figure 2a). Nonhierarchical clustering revealed drastic modifications of protein patterns during ripening. This was what expected confirming the quality of our data production and analysis. Interestingly, we observed a continuous variation of protein expression from ripening to full withering phase, indicating that an active protein modulation is still present after harvest. A one-way ANOVA analysis ($p \leq 0.05$) revealed 90 spots as being differentially expressed with an average ratio of 1.5 fold change in level comparing veraison to ripening and withering samples. The differential data set was also subjected to PCA to investigate inter- and intragroup relationships among

the six stages of berry development and to identify protein groups responsible for correlated variations (Figure 2b). 76% of the cumulative variance was represented by the first two principal components in PCA (PC1 61.9% and PC2 14.1%). Gel replicates cluster closely, indicating that the biological variation is responsible for the separation of the different samples. Along PC1, there is not an evident separation of the groups. In particular, data from the three withering stages are overlapped suggesting little changes in protein expression during the whole withering phase. A more clear partition exists along PC2, where protein samples belonging to the veraison group are evidently

distinct to those belonging to the ripening and withering groups, indicating a defined separation between the first phases of the berry development and the following physiological events in the fruit. Conversely, protein samples belonging to postveraison, ripening and withering groups were closely distributed along PC2, suggesting that proteins after veraison are modulated in a gradual and continuous manner, even after berry excision from the plant. As a confirmation of the PCA elaboration, we also evaluated the proteomic difference between ripening and veraison (R/V) and between withering and veraison (WIII/V). R/V and WIII/V were calculated as a percentage of total differentially expressed proteins. The protein variability observed during ripening (R/V) represented 65.43%, while the variability during withering (WIII/V) represented 64.19% of the total differential protein. The equivalence of the obtained values substantiated the finding that protein expression is still active during withering in a similar manner as during ripening.

Finally, a two-way hierarchical clustering analysis was performed to visualize the time-dependent expression patterns corresponding to the development and postharvesting berry response (Figure 2c). The clustering of columns, which indicates the distances among the six stages, showed that the bunch order reflects the sequential succession of samples. There is a clear difference between veraison and the two successive postveraison and harvest stages, which are grouped together. Vintage and withering stages again were closely clustered compared to the veraison group indicating that the most significant changes take place between veraison and the other stages. Moreover, the heat map of the differentially expressed proteins ($p \leq 0.05$) gave an overview of protein expression modification among the development and withering processes. In fact, proteins are grouped according to detailed horizontal branches, whose lengths represent a similar accumulation pattern. This analysis revealed two main groups of expression pattern in the veraison stage (37.4% proteins showed an increase and 62.6% proteins showed a decrease in abundance). Interestingly, the general trend of protein expression during veraison resulted inverted during withering phase (proteins accumulated during veraison showed a decrease in abundance in withering groups and vice versa), indicating the activation of specific metabolic pathways in these two different stages.

3.2. Identification of Protein Spots. Among the 90 differentially expressed spots analyzed by LC-ESI-MS-MS, 72 were identified as single proteins (Table 1). Most of the observed variations were related to energy and carbohydrate metabolism (25%), to oxidative and pathogen stress (30%), cytoskeleton (7%), and secondary metabolism (5%) (Figure 3).

Proteins Involved in Stress Response. Fruit ripening is characterized by oxidative processes, including the accumulation of hydrogen peroxide and peroxidized lipids in membrane, which entail reactive oxygen species (ROS) turnover.^{38–40} Contrasting data have been reported in the literature concerning the oxidative response in grape. Recent transcriptomics data demonstrated a significant induction of the oxidative response occurring at veraison which is actively modulated up to ripening process.¹⁵ Other authors, however, have not observed induction of oxidative stress response genes in mature berries, suggesting that the detoxification pathways are repressed during development.^{17,41} Tissue dehydration during withering is associated with increased cellular stress. Total soluble solids (BRIX), calculated from veraison to complete withering, have been estimated as an index of sugars and proteins accumula-

tion in the grape berry. During ripening, the BRIX value and berry weight increased, reflecting the active metabolism of this phase (Figure 4). During withering, the BRIX values continued to increase, whereas total berry weight fell. Thus, the dehydration process appeared to correlate with increases in sugar concentration. The stressing conditions of the withering phase caused the induction of stress response-associated proteins. Transcriptomics studies described the up-regulation of ROS scavenging enzymes during withering.⁵ In accordance with these findings, we observed an accumulation of glutathione peroxidase (GPOX), ascorbate peroxidase (APX), and protein disulfide isomerase (PDI) during the ripening and postharvest stages. APX and GPOX are responsible for H_2O_2 removal catalyzing its reduction to water; PDIs are oxidoreductases that catalyze the formation, reduction, and isomerization of disulfide bonds in newly synthesized secretory proteins. Moreover, we observed the glutathione-S-transferase (GST) down regulation in ripened tissues followed by a sharp increase in abundance during withering. A similar trend was recently observed in the water-deficit-stressed berry proteome.²⁰ GST is involved in the regeneration of glutathione, which maintains an intracellular reducing environment, influencing disulfide bond metabolism and preventing oxidation of thiols to disulfides. In addition, GST detoxifies compounds such as fatty acid peroxides, and it is also involved in the last step of anthocyanin accumulation by conjugating glutathione to cyanidin glucoside.⁴² Conversely, ROS-related species highly accumulated at veraison, such as polyphenol oxidase (PPO), peroxiredoxin (PRX 5), lipocalin temperature induced (TlnLi), and manganese superoxide dismutase (MSD), decreased in abundance during withering confirming previously reported observations.^{17,19,21} PPO catalyzes the production of *o*-quinones, compounds implicated in the browning reactions during defense response.⁴³ We identified three polyphenol oxidase isoforms at a lower molecular weight than expected (18 kDa instead of 67 kDa) possibly corresponding to putative degradation products. PRX 5, known as an important antioxidant protein, was highly expressed only at veraison together with MSD, which catalyzes the conversion of superoxide into hydrogen peroxide. TlnLi is reported to be involved in the transport of sterol molecules to the plasma membrane in response to stress conditions, increasing membrane fluidity at low temperature and maintaining the phospholipid structure at high temperature.⁴⁴ The role played by TlnLi may therefore be limited to the volume increase of berry occurring during veraison and it is negligible in the following phase of maturation.

This is the first time that many berry development proteins related to oxidative stress response have been described, showing distinguishable trends in ROS species accumulation between veraison and ripening/withering stages, which reflects the response of berry to different physiological conditions.

In accordance with previously published data,^{17–19,21} we observed a strong increase in the expression of pathogenesis-related proteins (PR) expression, such as thaumatin-like protein (TLP), class IV chitinases (Chit4), β -1,3-glucanase (Gluc β), and pathogenesis-related protein Bet v 1 (PRBetv1) at the onset of ripening, but a high modulation of these proteins was also observed during berry withering. The fact that most of the pathogen-related proteins are encoded by multigene families could explain the numerous spots identified as PR proteins isoforms, likely referable to post-translational modifications (PTMs), such as glycosylation or phosphorylation. Both Chit4 and Gluc β are known to exert catalytic activity, hydrolyzing

structural components of the cell walls of fungal hyphae.⁴⁵ Moreover, Gluc β plays a role in fruit ripening and softening since it has been detected as an abundant protein even in healthy tissues.^{18,46} An antifungal activity has been suggested for TLP which is probably associated with hyphal membrane permeabilization, in addition to the involvement in osmotic stress. The TLP family includes a number of variety-specific

isoforms, characterized by a variable molecular weights and extracellular or vacuolar localization.^{47–52} TLP itself is a potent sweet-tasting protein. Because of a small but detectable amount of these stable proteins, characterized by acid solubility, resistance to tannins precipitation and proteases degradation, several approaches for grape variety identification have been proposed, based on the analysis of proteins, such as TLP.⁵³

Table 1. Spots Identified by LC-ESI-MS/MS*

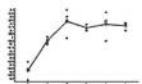
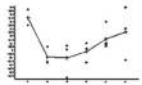
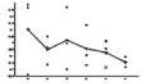
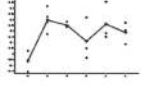

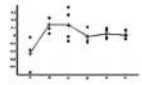
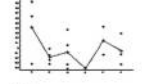
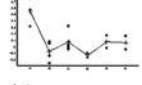
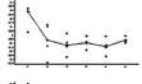
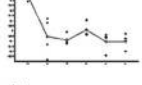
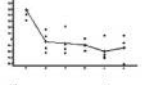
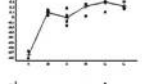
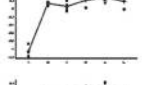
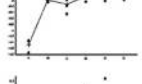
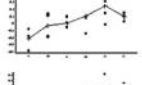
Spot no.	Protein name	Th MW / pI ^a	Exp MW / pI ^b	Total peptide / % coverage ^c	Score ^d	NCBI Accession ^e	Relative protein abundance ^f	Peptide sequence ^g
Stress								
1617	Glutathione peroxidase GPOX	18831/6.73	19972/6.24	4/52	235	gi 157356616		K.AEYPIFDK.I/R.GNDVLSIYK.G/K.IDVNGDSAPLY K.F/K.DQGLELAFPCNQF GAGEPGSNEIEK.F
1476	Glutathione-S-transferase GST	24884/6.16	23726/6.09	3/26	169	gi 157347785		K.VLDVYEAR.L/K.TADQAIIDVNLK.L/K.GLDFELVPV NLFAGEHK.Q
1715	Proxiredoxin PRX 5	7309/5.15	15825/5.33	5/53	416	gi 157342785		R.FALLVDDLK.V/R.FALLVDDLK.V/K.VIFGVPGFT PTCSVK.H/K.GIDELLVSNDFVVK.A/ K.VANVEAGGEFTVSSADDILK.A/K.FLADGSATYTHAL GLELDLSEK.G
311	Protein disulfide-isomerase precursor PDI	55951/4.93	58036/5.05	19/55	1185	gi 157336053		K.IVIVGVFPK.F/K.QSGPASAEIK.S/ R.GESSVTGPIV.R/L/ R.EADGIVEYLK.K/K.DPSNHPFVK.F/K.YHEVAEQYK. G/R.SKEDIIEFK.K/K.SAEDASSLVDNKK.SASGNIS QYEGDR.S/R.SDYDFVHTSDAK.F/K.SEPIPEVINEPV K.V/K.AASLSSHDPILAK.V/K.FVEESSVPTVLFNK.D K.VVADTLQEIFNSGK.N/K.LDATANDIPNDTFDK. G/K.DDQVPLVIQTNDSQK.Y/K.AMLFLDHSEELDAF K.S + Oxidation (M) K.LAPILDEVAISFENDADWIAK.L/K.GINFLLDLEASQ GAFQYFGLK.D
1176	Ascorbate peroxidase APX	27307/5.86	31147/5.82	6/53	467	gi 157337427		K.DIVALSQAHTLGR.C/R.QVFTQMLGSDK.D/K.ALLS DPAFRPLVEK.Y/K.YAADEDAFFEDYK.E/K.KPEELAH GANGLDIAVR.L/R.SGFEGPWTNPLIFDINSYF.K.E
1969	Manganese superoxide dismutase MSD	25325/6.79	24250/6.05	5/24	242	gi 147839972		K.YASEVYEK.E/K.NVRPYLK.N/K.ALEQLHEAMEK.G /K.NLTPVHEGGEPKK.G/K.LVETTANQDPLVTK.G
1704	Temperature induced Lipocalin TlnLi	21580/6.63	21282/6.15	8/43	405	gi 77744883		R.SYIEGTAYK.A/R.VLNETWSDGK.R/R.VLNETWSDG K/R.S/R.ATYTLLEADGTTVR.V/R.WYEIASFPFQPK.N /K.TTQDPPPEGEGPQDTK.G/R.QTHMDEEYMEIVE K.A/R.KTTQDPPPEGEGPQDTK.G
1757	Polyphenol oxidase PPO	67761/6.39	10340/5.25	6/17.6	168	gi 157328901		K.TTISSIGDFPK.A/K.EKENEVEELLIK.G/R.NSEFAGS FVNVPKH.H/R.AGGDDVTIGGIEFVSD.-/ K.FDVYINDEYYSVRPK.N/R.LAINELLELDGAEDDES VIVTIVP.R.A
1748	Polyphenol oxidase PPO	67761/6.39	12769/5.21	4/15.8	445	gi 157328901		K.TTISSIGDFPK.A/R.NSEFAGSFVNVPKH.H/R.AGGD DVTIGGIEFVSD.-/ R.LAINELLELDGAEDDESVIVTIVP.R.A
1754	Polyphenol oxidase chloroplast precursor PPO	67704/6.27	12682/5.11	4/13.5	109	gi 1172587		K.TTISSIGDFPK.A/K.EKEDEEEVLLIK.G/R.AGGDDVTI GGIEFVSD.-/ K.FDVYINDEYYSVRPK.N/R.FAINELLELDGAEDDES VIVTIVP.R.A
1227	Class IV Chitinase Chit4	28366/5.38	31802/4.97	4/22	436	gi 33329392		K.DYCSQLGVSPGDNLT.C.-/ /R.AINGAVECNGGNTAAVNAR.V/R.AAFLSALNSYSG FGNDGSTDANK.R/R.AAFLSALNSYSGFGNDGSTDA NKR.E
1211	Class IV Chitinase Chit4	28366/5.38	32020/4.87	4/22	435	gi 33329392		K.DYCSQLGVSPGDNLT.C.-/ /R.AINGAVECNGGNTAAVNAR.V/R.AAFLSALNSYSG FGNDGSTDANK.R/R.AAFLSALNSYSGFGNDGSTDA NKR
1171	Class IV Chitinase Chit4	28366/5.38	32718/5.08	4/22	400	gi 33329392		K.DYCSQLGVSPGDNLT.C.-/ /R.AINGAVECNGGNTAAVNAR.V/R.AAFLSALNSYSG FGNDGSTDANK.R/R.AAFLSALNSYSGFGNDGSTDA NKR
1377	Class IV Chitinase Chit4	21021/5.38	30798/5.08	7/22	400	gi 147855950		K.EIVIEEEK.K/K.EEIVMEER.E/K.EKEVIEEEK.K/ R.EATEAVAAAAEPKP.-/K.VIEYEASSTEIK.T/ K.YGPQLVSGPVLFLFEK.V/K.VSTFIVTEENEEELPPP TTNITGEEESGK.E
1030	Beta 1,3-glucanase Glucβ	36676/8.45	38131/5.79	6/30	98	gi 157348466		NGNNLPAGEVVALYNQYR/VSTADTGMVGSYPP SSGSFKNLFDAILDAVY/SALER/VWSESGWPSAGGT QTTVDNARTYNSLIQHK/HWGLFLPK/QPK/ESPI FNQGR

Table 1. Continued

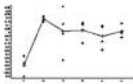
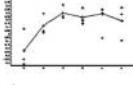
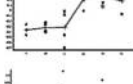

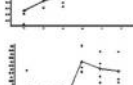
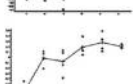
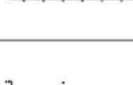
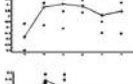
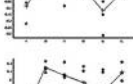
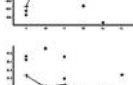
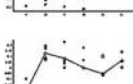
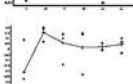
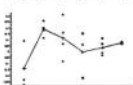
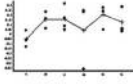
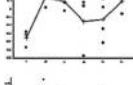


Spot no.	Protein name	Th MW / pI ^a	Exp MW / pI ^b	Total peptide / % coverage ^c	Score ^d	NCBI Accession ^e	Relative protein abundance ^f	Peptide sequence ^g
Stress								
1892	Pathogenesis-related protein Bet v 1 family PRBetv1	17265/5.12	17037/5.36	8/68	420	gi 147865627		K.ILETETK/A.K.DIESHLNA-/ K.ETVDQDEENR/S.R.SQAHHLPN/CSOK/I.K.HWSLT VGENSESIK/E.K.GEGCLVIWTIEYK/A.K.IEVHEGDW ETQGSVK/H.K.ASEGQDPHNCLEFSVNTK.D
1593	Putative ripening-related protein GRIP	17172/5.67	10543/5.62	2/16	77	gi 157352972		K.VWSPDGGSIYK/N.K.NVEIIQEGGPGTIK.K
1393	Osmotin-like protein OLP	24828/4.56	26083/4.81	4/32	357	gi 1839046		R.CPDAYSYPK/D.R.TNCNFDASGNK/C.K.TTGGCN NPCTVFK.T/R.GISCTADIVGECPAALK.T/K.TDEYCCN SGSCNATTYSEFFK.T
1362	Absisic stress ripening protein ASR	13122/6.81	24774/5.56	1/20.9	69	gi 584786		K.IEEIEAAAAVAGGAFHEHHEK.K
1439	Thaumatin-like protein TLP	24947/4.94	23944/4.86	5/54	449	gi 7406716		R.CPDAYSYPK/D.R.TNCNFDASGNK/C.K.TRPCDAY SYPK/D.K.TTGGCNNPCTVFK.T/R.GISCTADIVGEC PAALK.T/K.TDEYCCNSGSCNATDYSR.F
1413	Thaumatococcus protein TLP	24812/4.67	30230/5.38	4/32	207	gi 157357182		R.CPDAYSYPK/D.K.TTGGCNNPCTVFK.T/R.GISCTA DIVGECPAALK.T/K.DDOTSTFTCTAGTYEWFVCF-/
1357	Putative thaumatin-like protein TLP	24947/4.97	24555/5.00	12/54	907	gi 7406716		R.TSCTFDANGR/G.K.APGGCNNPCTVFK.T/R.CPDAY SYPQDDK.T/K.TSLFTCTSGTNYK.V/K.CITYVWAAA SPGGGR/R.K.DRPCDAYSYPQDDK.T/R.GIQCSADIN GQCPSELK.A/R.LDSGQSWITVNPPTTNR.I/R.RLD SGQSWITVNPPTTNR.I/K.TNEYCCTDGPSCGPT TYSK.F/R.CPDAYSYPQDDK.TSLFTCTSGTNYK.V/R.G IQCSADINQCPSELKAPGGCNPCTVFK.T
Energy and carbon metabolism								
594	Phosphoglycerate kinase PGK	50166/6.64	50808/5.26	2/20	107	gi 147843756		K.DVTIIGGDSVAVEK.V/ K.LVTALPDGGVLLLENV.R.F
595	Phosphoglycerate kinase PGK	50166/8.26	50571/5.41	2/7.1	107	gi 147843756		K.DVTIIGGDSVAVEK.V/ K.LVTALPDGGVLLLENV.R.F
414	UTP-glucose-1-phosphate uridylyltransferase UGP	51389/6.64	57019/5.82	5/13.8	311	gi 157353934		K.MEIPNPK.E + Oxidation/ K.GGLTISYEGK.V/ R.VVVDDFSPLSK.G/R.FFDNAIGINVR.S/ R.SAVAGLDQISENEK.S
1599	Triosephosphate isomerase TPI	27466/6.34	26913/6.06	8/56	573	gi 147784332		R.IYIGSVSGANCKE.K.VIACVGETLEQR.E/R.ESGS TMEVVAQTK.A + Oxidation (M)/ R.LLLNESNEFYGEK.VK.VATPAQAEVHSELN/I.K. YSNWANWVLAYPEVWAGTGK.V/R.NWFQANTSPEV AATIR.I/K.IVSTLNAGEVPSGDVVEVVSPPFVFLPLV K.S K.HIANLAGNK.R.R.IEEELGSAAYAGAK.FK.VNQIGS VTESIAVK.M.VVIGMDVAASEFYDNK.D + Oxidation (M)/ R.AAVPSGASTGIYEALER.D.K.YGQDATNVGDEGGF APNIQENK.E/K.YGQDATNVGDEGGFAPNIQENK.E
406	Enolase ENO	47769/6	56727/5.65	72/21	451	gi 157355881		K.ELLEWGRS.V/R.IYVPEGQPLR.S/ K.CNTTAYENVHR.V/K.VVCEEDLINIETATGSK.K/ K.VTNQMQLAAVEAAAFNLK.A/ K.NIGCCNELNAGYAADGYAR.S
178	Pyruvate decarboxylase PDC	63487/6.09	60524/5.60	6/18	371	gi 10732644		K.LQSSLPEVNIK.V/R.LSGTGSEGATIR.V/ R.SMPTSAALDVVAK.H + Oxidation (M)/ R.YDYENVDAKAK.E
184	Phosphogluco-mutase PGluM	63656/5.81	60655/5.56	4/13	242	gi 157338975		K.VSPEWAEYTVR.T/R.LASINVENVEGNR.R
735	Fructose-1,6-bisphosphate aldolase ALD	39005/8.03	40760/5.69	2/12.6	116	gi 147781269		R.SSIFDAK.A/R.SSIFDAK.AK.AATYEQVK.AK.KWIS APSK.D/K.AAIKEESEK.MK.YDSVHGQWK.H/R.VPT VDVSVDLTVR.LK.GILGYTEDDVVSTDFGDN.R.S
755	Glyceraldehydes-3-phosphate dehydrogenase G3PDH	34733/6.62	44851/6.44	7/26	416	gi 157327869		K.IYEGEFK.Y/K.LVDFALDSGK.V/R.IDQLQLLK.G/ K.GVDAQIAGSGGR.M/K.SLEYEDFK.F/ R.YENDWEVVK.R/R.TSGEYLHNGVR.T/ R.GWDAQVLGEAPHK.F/K.SLEYEDFKFDR.V/ K.LPNHYLVSPPEIER.T/ R.DVLDGSSVGFVTELDLAK.L/ R.VNLPNGDMVGHGTGDIATVACK.A + Oxidation (M)/ R.SGYFDPMSMEYVEIPSDSGITFNKPK.M + Oxidation (M)
175	2,3-bisphosphoglycerate-independent phosphoglycerate mutase PGlyM	60385/5.4	60655/5.52	13/36	804	gi 157353414		

Table 1. Continued

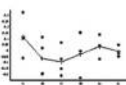
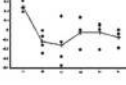

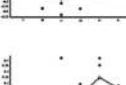
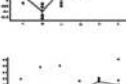

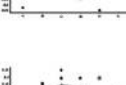
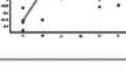
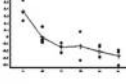
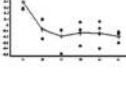
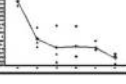
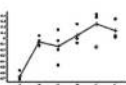
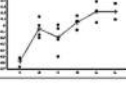
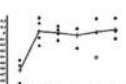
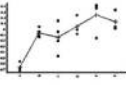
Spot no.	Protein name	Th MW / pI ^a	Exp MW / pI ^b	Total peptide / % coverage ^c	Score ^d	NCBI Accession ^e	Relative protein abundance ^f	Peptide sequence ^g
<i>Energy and carbon metabolism</i>								
290	Vacuolar invertase I GIN-1	71786/4.6	65000/5.01	5/20	334	gi 1839578		R.DPTTMVVGADGNWR.V + Oxidation (M)/ R.ILYGWISGDISSDLK.K/K.TGYLLWPREEVSLR .TK.YENNPVMPVPPAGIGSDDFR.D + Oxidation (M)/ R.HDYALGEYDPMTDTWTPDDPELDVIGLR.L + Oxidation (M)
276	Vacuolar invertase I GIN-1	71786/4.6	65509/4.77	9/20	563	gi 1839578		R.TAFHFQPEK.N/K.GWAS R.DPTTMVVGADGNWR.V.LQISPR.T/ R.DPTTMVVGADGNWR.V/ R.ILYGWISGDISSDLK.K/ R.DMIHWL.YL.PLAMVPDR.W + 2 Oxidation (M)/ K.TGYLLWPREEVSLR.T/ R.ILYGWISGDISSDLK.K.G/ K.YENNPVMPVPPAGIGSDDFR.D + Oxidation (M)/ R.HDYALGEYDPMTDTWTPDDPELDVIGLR.L
275	Vacuolar invertase I GIN-1	71786/4.6	66912/4.60	9/20	610	gi 1839578		R.TAFHFQPEK.N/K.GWASLQISPR.T/R.DPTTMVVGADGNWR.V/R.ILYGWISGDISSDLK.K/R.DMIHWL.YL.PLAMVPDR.W + Oxidation (M)/ K.TGYLLWPREEVSLR.T/R.ILYGWISGDISSDLK.K.G.K.YENNPVMPVPPAGIGSDDFR.D + Oxidation (M)/ R.HDYALGEYDPMTDTWTPDDPELDVIGLR.L
1345	Alcohol dehydrogenase ADH	28017/5.74	29313/5.62	10/55	856	gi 157356344		K.FIDYVMSK.MR.AIVADIQAEK.G/K.GQLVAESIGLH R.CK.VAITGGASGIGETAR.HK.DVADAVFLASDN SK.FR.YILCDVTDEQVK.A/K.GSICTASVSASTGSD K.FK.FVTGHNLDGGYPY.-/ R.VNSVSPGAVATPLLCDK.F/K.EKDVAFLASDN SK.FK.FQMSATEVNEFFQYMSLK.G
792	Pyruvate dehydrogenase PDH	36084/4.99	44330/5.25	4/19	199	gi 157360513		K.DGISAEIILR.S/K.VLSPYSESDAR.G/R.SIRPLDTP INASVR.K/R.DALNSALDEMSADPK.V + Oxidation (M)
408	Aldhyde dehydrogenase AD	58640/6.54	55985/5.79	9/30	626	gi 157350789		K.LAFTGSTATGK.I/K.AFDEGPWPR.M/ K.IGPALACGNITVLK.T/R.SGVENGATLETGGER.F/ K.TAEQPLSALYASK.L/R.TFVHESIYDEFVEK.A/ K.AGIEQGPQSDQFEK.I/ R.TGNVASVAEGDAEDVNR.A/ K.HNDEIAALETWNGKPFQAAK.A/ R.ANATSYGLAAGVFTQNLDTANTLTRA
585	Succinyl-CoA SCS	45829/5.8	49044/5.33	10/32	670	gi 147782941		K.TIGDVFPK.E/K.MLGQILVTK.Q + Oxidation (M)/ R.LEGTNDVQGR.R.K.GVAVGSIEEVR.K/R.SSAGPIIA CR.K/R.LEGTNDVQGR.I/K.CDIASGIVNAEK.E/R.LNI HEYQGAELMSK.YK.VPIDVFQGITDEDAK.VIK.ESG MALITAEIDDDAAEK.A + Oxidation (M)/ K.LHGGETPANFLDVGNGASESQVVEAFK.I
<i>Photosynthesis</i>								
1070	Manganese-stabilising protein/ photosystem II MnSpPSII	33441/5.87	36647/5.27	10/51	633	gi 147791852		R.VPFLFTIK.QR.LTYDEIQSK.T/K.R.LTYDEIQSK.T/K.F GGEFLVPSYR.G/K.FCLEPSTFTK.A/R.GGSTGYDNA VALPAGGR.G/K.DGIDYAAVTQLPGGER.V/K.GTGT ANQCPTIDGGVDSFAFK.S/R.L.TYTLDEIEGPFVSSD GTVK.F/K.SKPETGEVGVFESIQPSDSDLGAK.T
1078	Manganese-stabilising protein/ photosystem II MnSpPSII	33441/5.05	36647/5.33	12/38	768	gi 147791852		R.GDEEELKK.E/R.VPFLFTIK.QR.LTYDEIQSK.T/K.NA PPEFQNTK.L/K.R.LTYDEIQSK.T/K.FGGEFLVPSYR.G/ K.FCR.GGSTGYDNAVALPAGGR.G/ILEPSTFTK.AK. DGIDYAAVTQLPGGER.V/K.GTGTANQCPTIDGGVDSFAFK.S/R.L.TYTLDEIEGPFVSSDGTVK.F/K.SKPET GEVGVFESIQPSDSDLGAK.T
1063	Manganese-stabilising protein/ photosystem II MnSpPSII	33441/5.87	36516/5.19	7/29	371	gi 147791852		R.GDEEELKK.E/R.GDEEELKK.EK.ENIKDASSSTGK.I/ K.R.LTYDEIQSK.T/K.FGGEFLVPSYR.G/R.GGSTGYD NAVALPAGGR.G/K.DGIDYAAVTQLPGGER.V
<i>Lipid metabolism</i>								
1267	Dienelactone hydrolase DLH	26307/5.22	30099/5.26	3/26.4	159	gi 147767003		K.AYVAGPSDSK.HK.APIAVLGAEDIK.AK.SDYIQSA V.LLHPSR.V
1194	3-ketoacyl-(acyl-carrier-protein)- reductase ACPR	28017/5.74	29313/5.62	3/16	170	gi 157356344		R.AIVADIQAEK.G/K.VAITGGASGIGETAR.HK.FVT GHNLDVGGYPY.-
<i>Secondary metabolism</i>								
621	Chalcone synthase CHS	43163/6.18	50877/5.50	2/25	66	gi 12002451		K.ENPHMCAYMAPSLDAR.Q + Oxidation (M)/ K.ENPHMCAYMAPSLDAR.Q + Oxidation (M)
1266	Chalcone-flavone isomerase CHI	25295/5.26	30230/5.23	2/18.4	108	gi 1705761		R.DWVTGPFKEK.F/ K.LLLEAVLESIGK.H
916	Kynurenine formamidase KF	30078/5.15	40619/5.37	6/26	313	gi 147838052		R.LPGAEGAPIR.Q/R.EVLVESLK.L/R.WLVENTDIK.L/ K.EFESDYAGFTEDGAR.WK.KEFESDYAGFTEDGAR .W/R.IFDITHPYTPNMTFGTDEGIGEWLEK.S + Oxidation (M)

Table 1. Continued

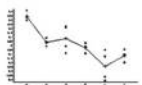
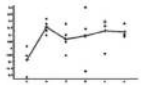
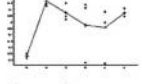
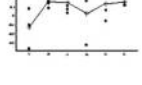
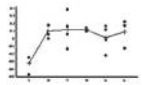
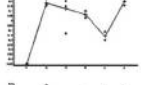
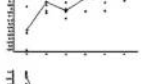
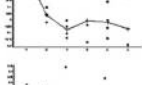
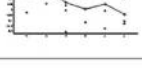

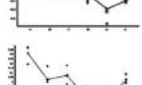

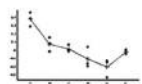
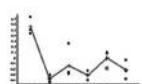
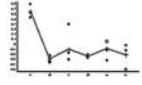

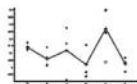
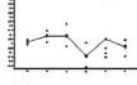
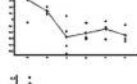
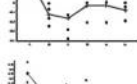
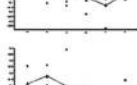
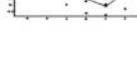
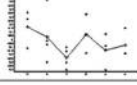
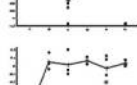
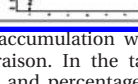
Spot no.	Protein name	Th MW / pI ^a	Exp MW / pI ^b	Total peptide / % coverage ^c	Score ^d	NCBI Accession ^e	Relative protein abundance ^f	Peptide sequence ^g
<i>Secondary metabolism</i>								
1380	Flavodoxin Quinone reductase FaQR	23994/5.51	25472/5.64	2/20	102	gi 147811922		K.GAESVEGVEVK/LK.AFLDAGALWR.T
<i>Aminoacid metabolism</i>								
711	Type 1 glutamine amidotransferase GAT	42098/5.45	42098/5.45	2/9.8	60	gi 157347768		K.ALGGITIGSDK/R.APEYLALNEK.V
400	Aspartate aminotransferase AsAT	59699/5.62	57163/5.30	5/13	63	gi 157339869		K.DGILSSLR/R.K.GFMEEFR.D + Oxidation (M)/ R.CTILPQEDK.I/K.AEGAMYLFPRI + Oxidation (M)/ R.GGYMEVTGFGADVRE + Oxidation (M)
724	Glutamine synthetase cytosolic isozyme 1 GLS	39403/5.79	46200/5.73	9/41.6	612	gi 1707955		R.NDGGFEVK/K/R.TLSPGVSDPAK/L/ R.NDGGFEVKK/A/K.EHIAAYEGNER/R/ K.VIVEYIWWGGSGMDLR/S/ R.HTADINTFLWGVANR/G/ R.GNNILVMCDTYTPAGEIPTNKR + Oxidation (M)/ R.GNNILVMCDTYTPAGEIPTNKR.C/ K.IFSPDVAEVPWYGIEQYTLQK.E/ K.WNYDGSSTGQAPGEDSEVILYQAIK.D
<i>Cytoskeleton</i>								
610	Actin ACT	41796/5.23	50650/5.38	6/19.9	306	gi 18532		K.VWAPPERK.Y/K.AGFAGDDAPR.A/R.AVFSPVGRP R.HK.DAYVGDEAQSQR.G/K.GEYDESGPSIVHR.K/K. DLYGNIVLGGSTMFLGIADR.M + Oxidation (M)
620	Actin ACT	41796/5.23	49402/5.45	6/29	418	gi 18532		K.VWAPPERK.Y/K.DAYVGDEAQSQR/R/ K.DAYVGDEAQSQR.G/K.GEYDESGPSIVHR.K/ K.LAYVALDYEQLETA.S/ K.DLYGNIVLGGSTMFLGIADR.M + Oxidation (M)
1412	Actin ACT	20192/4.86	30667/5.41	4/37	350	gi 14133878		R.GYMFITTAER.E + Oxidation (M)/ K.NYELPDGQVITGAER.F/K.LAYVALDYEQLETA.S R.VAPEEHFVLLTEAPLNPK.A
222	Actin ACT	41796/5.23	62317/5.51	3/30	150	gi 18532		K.AGFAGDDAPR.A/K.DSYVGDEAQSQR/R/ K.DSYVGDEAQSQR.G
412	Tubulin alpha TUB-α	50228/5.71	54631/5.22	10/30	700	gi 6723478		K.DVNAVAATIK.T/K.EIVDLCLDR.I/R.TIOFVDCPTG FK.C/R.SLDIERPTYTNLR.L/R.AVFVDEPTVIDEVR. T/R.AVCMISNSTSVAEVSFR.I + Oxidation (M)/ K.CGINYQPPTVPPGGDLAK.V/K.TVGGDDAFNTFFS ETGAGK.H/R.AFVHWYVYEGMEEGFSEAR.E/R.FD GALNVDTVFQTNLVPYPR.I
<i>Cell wall structuring</i>								
1087	Xyloglucan endotransglycosylase XET	33501/5.91	37345/6.00	3/21	189	gi 147771556		K.YQYLFGR.V/R.VTFYIDEVPIR.V/K.SRYPVTPECEVA GL-/K.LQPMGWSTLWEADDWATR.G + Oxidation (M)
258	Pectate lyase PL	58732/5.99	62805/5.46	2/3.2	49	gi 32489378		K.IKVLQR.K/K.IKVLQR.K
235	Pectate lyase PL	58732/5.99	63296/5.42	2/3	49	gi 32489378		K.IKVLQR.K/R.NTLSSVLLPPK.K
<i>Protein synthesis, folding, transport and degradation</i>								
254	RuBisCO binding protein RuBP	61787/5.06	58822/5.11	11/28	800	gi 157346726		LADAVGLTLGPR.G/K.DSTTIADAASK.D/ R.NVVLDEFGSPK.V/K.VGAATELEDR.K/ R.GYSPQFVTNPEK.L/K.YENLVEAGVIDPAK.V/ K.TNDSAGDGTITASVLAR.E/R.AIELADAMENAGAALI R.E/R.SPLLVAEDVTGEALATLVNKL
212	RuBisCO binding protein RuBP	61787/5.06	58866/5.09	11/22	703	gi 157346726		K.LIAEFENAR.VIK.DKLEDADER.L/K. K.LIAEFENAR.VIK.DKLEDADER.L/K.ARPVEGGDDIK. AK.LADAVGLTLGPR.G/K.DSTTIADAASK.D/K.VGAA TETELED.R/K.R.GYSPQFVTNPEK.L/K.YENLVEAGVI DPAK.V/K.TNDSAGDGTITASVLAR.E/R.AIELADAME NAGAALIR.E/R.SPLLVAEDVTGEALATLVNKL
1910	Alpha-crystallin-type heat shock protein HSP	16530/5.81	16463/5.75	2/11	67	gi 157344153		R.II.QISGDR.SIK.AEVKPKDVK.A
1857	Alpha-crystallin-type heat shock protein HSP	17041/5.3	17386/5.55	2/6	114	gi 157344152		K.ADLPGVK.K/K.AEVKPKDVK.A

Table 1. Continued

Spot no.	Protein name	Th MW / pI ^a	Exp MW / pI ^b	Total peptide / % coverage ^c	Score ^d	NCBI Accession ^e	Relative protein abundance ^f	Peptide sequence ^g
<i>Protein synthesis, folding, transport and degradation</i>								
1279	Putative transcription factor TF	16693/5.68	23988/5.72	2/30	156	gi 14582465		K.HLEHLGELGVAAGAYALHEK.HK.IEEIEIAAAAVG AGGFATHEHEK.K
873	Ribosomal_L10 RPL10	34325/5.23	41167/5.54	5/28	321	gi 147843260		K.VGSSEALLAK.LK.GTVEITPVELIR.K.K.FAVAVAP VAAADAGGSAAPPK.EK.NVLSVAVATEYSPQADK.V /K.LCQLDEYTIQIIAADNVGSQLQNIIR.K
951	Proteasoma alpha subunit type I Pa	31035/5.02	39310/5.27	6/28	430	gi 147856362		R.FGTQNSR.EK.THVLVACNKK.A.R.LFQVEYAME AVK.QK.VDDHGVIAAGLTADGR.V.R.NQYDVTVTW SPAGR.L.R.SECINYSFTYELSPVGR.L
297	Protein tyrosine kinase PTK	90624/5.34	56465/4.63	2/8	72	gi 157338176		K.TTNILLDENFVAK.VIK.GMLDQIMDPNLVGK.V + Oxidation (M)
270	ATP synthase CF1 alpha subunit FatpA	55437/5.26	57905/5.38	8/20.9	472	gi 91208887		R.GEISASESR.L/R.ADEISNIIR.E.R.LIESPAGIIR.R/ R.HTLIYDDLK.QK.IAQIPVEAYLGR.VIK.ASSVAQV VTFQER.G.R.EAYPGDVFYLSR.LK.IVNTGTVLQV GDGIAR.I
410	F1 ATP synthase beta FatpB	60004/5.84	55941/5.33	17/49	1722	gi 147838606		K.VVDLLAPYOR.G.R.TIAMDGTGLVR.G.R.IINIGEP DER.GIK.ESITSGVLDGK.Y.K.AHGGSFVAGVGR .T.R.VGLTGLTVAEHFR.D/R.VLNTGSPITVPVGR.A/K. TVLIMELINNVAK.A/R.FTOANSEVSALLGR.I/K.CALVY GOMNEPPGAR.A/R.LVLEAQHLGENMVR.T/R.DAEG QDVLIFDNIIR.F/R.QISELGYPAVDPLDSTR.M/K.N LQDIILGMDLSEDDK.L + Oxidation (M)/ R.EAPSFVDQATEQQILVTGIK.VIK.YDDLSEGSFYMN GGIEEVIAK.A + Oxidation (M)/ K.ITDEFTGAGAGSVCCQVIGAVDVR.F/K.NLQDIILG MDELSEDDKLTVAR.A
<i>Storage</i>								
731	Cupin 2	53304/8.58	46294/5.24	4/22.3	301	gi 157350579		R.VEGGLQAVLPFR.G.R.GLLPSYVNAQQLMYFVQG R.G + Oxidation (M)/ R.QLIVSVLDTSNDANQLDFQPR.R/R.EVEEGDVFV PVGTH-FIYNNGR.Q/R.IQSEAGVTEVFDHNEQFQ CAGAVVR.Y
<i>Unknown function</i>								
791	DUF-642	40651/5.77	44330/5.18	4/22	273	gi 157339642		K.YIDSHFVSPQEK.R/K.QGDMILLWPEGAFAVR.L/R .SDDYASL.CGPVLDVKK.L/K.TYALSFVSGDASNSCEG SMVVEAFAGR.D + Oxidation (M)
572	DUF-642	40651/5.77	50135/5.40	6/19	319	gi 157339642		K.RAVELVAGK.EK.ESAIQVAR.T/K.YIDSHFVSPQ EK.R/K.QGDMILLWPEGAFAVR.L + Oxidation (M)/ R.SDDYASL.CGPVLDVKK.L

*Proteins were considered as differentially expressed when a 1.5-fold increased or decreased accumulation was statistically confirmed by one-way ANOVA with a p value ≤ 0.05 . The fold change was calculated comparing all stages versus veraison. In the table we reported: theoretical (a) and experimental (b) molecular weight expressed in kDa and isoelectric point, number of total peptide and percentage of amino acid coverage (c), ion score (d), NCBI accession number (e), and peptide sequences (g). The variation of berry protein abundance during the six stages of ripening/withering (indicated as A, B, C, D, E, and F on the X axis) is shown by linear graphic representation of average normalized volumes (standard log abundance on the Y axis) calculated on the basis of the 2D-DIGE protein map analyzing 100 μ g berry protein (f).

A different expression trend was observed for the osmotin-like protein (OLP), which was selectively accumulated in the withering stage. OLP is described as a "thaumatin-like protein" associated with the osmotic adaptation in plant cells.⁵⁴ The expression of OLP in various plant species has been reported in response to pathogen infection^{55–58} or environmental stresses.^{55,59,60} The high OLP expression levels during withering are likely due to the dehydration stress associated with an increased hexose concentration.⁶¹

We also found a significant presence of the abscisic stress ripening protein (ASR), which showed a variable trend during berry development, with a strong accumulation during ripening, followed by a small decrease in abundance in the last stage of withering. Water deficit induces ASR expression and, during grape ripening,⁶² ASR enhances skin pigmentation accelerating anthocyanin biosynthesis⁶³ and induces the accumulation of protective proteins during water stress and tissue desiccation.⁶⁴ A grape ripening related protein (GRIP), whose function has yet to be elucidated, was also identified as overexpressed during

maturation, while a gradual decrease in its abundance was observed during withering.

Protein Associated with Energy and Carbon Metabolism.

After veraison, a general activation of glycolytic pathway was observed (Figure 5) in accordance with other studies.^{19,21} The sucrose, transported by floem and accumulated in cell apoplast, can be hydrolyzed or transported inside the cytoplasm, where it enters the glycolytic pathway and is converted into pyruvate. The expression of vacuolar invertases encoding genes and the synthesis of the corresponding products occur early in berry development, preceding the hexose accumulation resulting from sucrose hydrolysis.⁶⁵ This evidence is confirmed by our observation of a progressive decrease in abundance of glucose vacuolar invertase 1 (GIN-1), suggesting that sucrose transport to vacuole may have decreased during berry maturation.

In relation to the increased catabolism, we identified several key catabolic enzymes which accounted for 21% of all identified proteins, namely, UTP-glucose-1-phosphate uridylyltransferase (UGP), phosphogluco-mutase (PGluM), fructose-1,6-biphos-

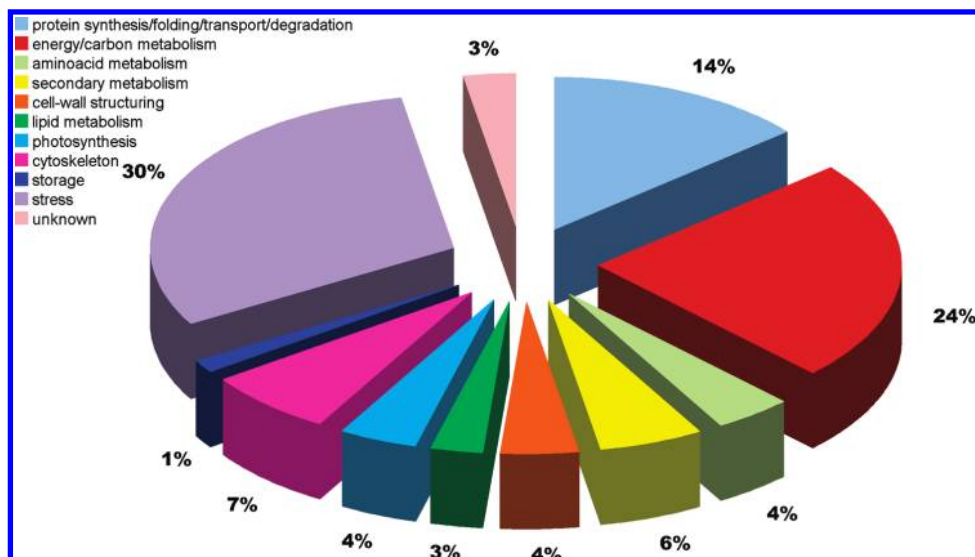


Figure 3. Functional distribution of the identified proteins in the grapevine berries. Proteins were classified on the basis of data available in the literature and using the information available in the Swiss-Prot/TrEMBL and Gene Ontology databases.

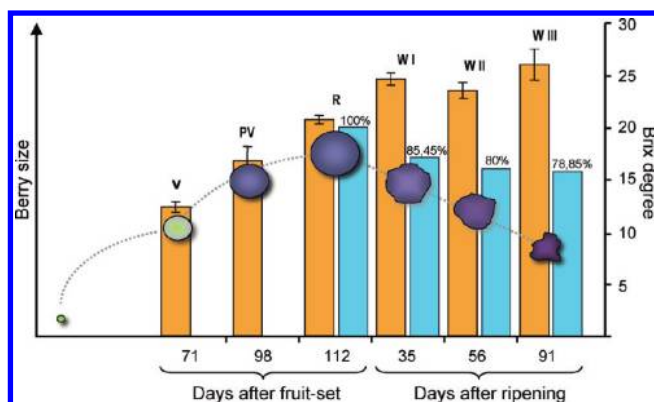


Figure 4. Brix degree and dehydration of the six sampling time-points. Brix (yellow bars) are expressed as mean \pm s.d. of the three biological replicates. Water loss (blue bars) was calculated as percentage of weight loss, using ripening berries (R) as a reference. V: veraison, PV: postveraison, R: ripening, WI: withering phase I, WII: withering phase II, WIII: withering phase III.

phate aldolase (ALD), glyceraldehyde 3-phosphate dehydrogenase (G3PDH), phosphoglycerate kinase (PGK), 2,3-bisphosphoglycerate-independent phosphoglycerate mutase (PGI_M), enolase (ENO), which was sequentially up-regulated. Triose-phosphate isomerase (TPI), which catalyzes the interconversion of dihydroxyacetone phosphate and D-glyceraldehyde-3-phosphate, also showed a slight decrease in abundance during the ripening process.

The trichloroacetic acid cycle seemed to be directly activated by the pyruvate that is converted to acetyl-CoA by mitochondrial pyruvate dehydrogenase (PDH), which was more abundant in the mature berry. Moreover, the accumulation of cytosolic pyruvate promotes the production of ethanol through the serial up-regulation of pyruvate decarboxylase (PDC) and alcohol dehydrogenase (ADH) involved in alcoholic fermentation.⁶⁶ We observed a further ADH expression increase during withering, providing evidence of the shift from aerobic metabolism to anaerobic fermentation. Our data also suggest that ADH, implicated in the interconversion of the aldehyde and alcohol forms of flavor volatiles such as carotenoid- and shikimate-derived compounds, accumulates in the fruit during

ripening, likely playing an important role in flavor development.^{67,68} As a common trend, glycolytic enzymes showed a sharp expression peak after veraison followed by a new clear rise during the last withering stage. Among the enzymes involved in the trichloroacetic acid cycle, aldehyde dehydrogenase (AD) and succinyl-CoA synthetase (SCS) showed a strong activation of expression immediately after veraison, in agreement with the increase of pyruvate decarboxylase and alcohol dehydrogenase in mature berry.

Protein Associated with Secondary Metabolism. Enzymes involved in the anthocyanin pathway have rarely been analyzed by 2-DE due to their low abundance;^{18,19,69} however, chalcone isomerase (CHI) and chalcone synthase (CHS), both members of this pathway, were identified as differentially expressed in this study. The sharply increased abundance of these proteins immediately after veraison suggests an activation of the flavonoid pathway, most likely as a consequence of the pigments' accumulation in the skin. The observed plateau of expression during withering is in accordance to transcripts trends^{5,7} and can be related to water stress, which has been demonstrated to activate flavonoid structural genes and to induce accumulation of phenylpropanoid skin-specific proteins in other studies.^{20,70} The high level of polymorphisms within the CHS gene family has also been used to discriminate grapevine clones.⁷¹

A differential expression of flavodoxin quinone reductase (FaQR) was observed. Different metabolic functions have been proposed for this protein. A fast activation of FaQR transcription as auxin response has been reported.⁷² This enzyme, which is thought to be involved in aroma development, accumulated during strawberry maturation.⁷³ A further role of FaQR relates to the involvement of flavodoxin in the photosynthetic process as electrons shuttle from Photosystem I to flavodoxin-NADP(H) reductase.⁷⁴ A gradual decrease in abundance of FaQR during berry ripening and withering was observed. This evidence may suggest a major role of the detected grape FaQR in photosynthesis rather than in aroma compounds synthesis.

The expression of kynurenine formamidase (KF) decreased during maturation and remained unvaried during withering. KF hydrolyzes the formylkynurenine, an intermediate in the tryptophan oxidation pathway, into kynurenine. This com-

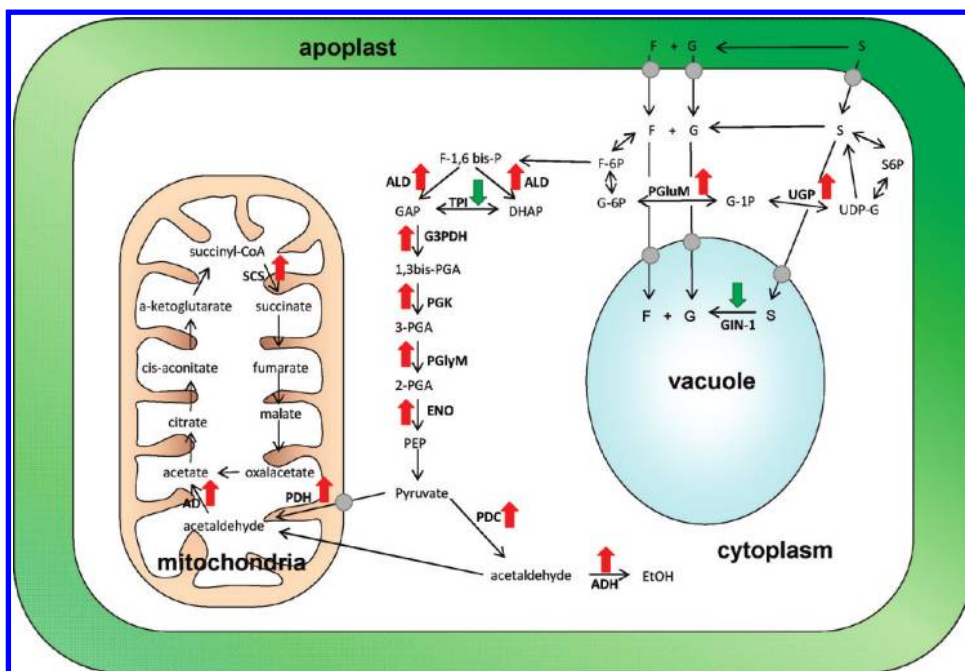


Figure 5. Scheme of the enzymes involved in sugar metabolism and their connection with TCA cycle. Protein expression variation was evaluated comparing ripening and postharvesting versus veraison stage. Red and green arrows indicate an increase and decrease in protein abundance, respectively. GIN-1: vacuolar invertase; UGP: UDP-glucose-pyrophosphorylase; PGLuM: phosphogluco-mutase; ALD: aldolase; TPI: triosephosphate-isomerase; G3PDH: glyceraldehyde-3-phosphate dehydrogenase; PGK: phosphoglycerate kinase; PGlyM: phosphoglycerate-mutase; ENO: enolase; PDC: pyruvate decarboxylase; ADH: alcohol dehydrogenase; PDH: pyruvate dehydrogenase; AD: aldehyde dehydrogenase; SCS: succinyl-CoA synthetase.

pound is reported as one of the potential precursors of 2-aminoacetophenone, which is thought to affect the wine aroma causing an “untypical aging off-flavor”.⁷⁵

Cell-Wall Modifying Enzymes. Modification of cell wall polysaccharides properties during grape berry softening is a complex process, in many cases controlled by the activity of a small amounts of enzymes.⁷⁶ During cell expansion and elongation, characterized by a dynamic loosening and reinforcement of the cell wall, hydrolases have a crucial role in the control of the weakening process.^{77,78} Our analysis revealed the differential expression of two wall hydrolases, namely, pectate lyases (PL) and xyloglucan endotransglycosylases (XET), with opposite trends during berry maturation. The profile revealed an accumulation of XET after veraison. This observation is in accordance to the expected trend of enzymes involved in berry softening.^{18,76} Alternatively, a reduced expression of two isoforms of PL during ripening was observed. PL is responsible for the cleavage of pectate, yielding oligosaccharides with 4-deoxy- α -D-mann-4-enuronosyl groups at their nonreducing ends (EC 4.2.2.2). Although the preferential role described for this enzyme is related to maceration and soft decomposition of plant tissue, in grape berry the major involvement of PL is likely related to structural modifications in early berry development. For both XET and PL, a reduction of the expression was observed after harvesting. This may be due to the reduced cell turgor, which is a consequence of water loss, resulting in a down-regulation of enzymes involved in cell wall dynamic depolymerization. These data may suggest that during the first phase of withering the biochemical changes that affect cell expansion are inhibited,⁷⁹ although we also observed a new accumulation of both cell wall enzymes in the late withering. At this stage, their expression may be induced

by mechanical stress factors that require adaptive modification as a consequence of tissue tensile strength or flexibility changes.⁸⁰

Protein Involved in Lipid Metabolism. In mature and withered berries, we observed an accumulation of dienelactone hydrolase (DLH), the third enzyme involved in the halocatechol branch of the P-ketoadipate pathway, which catalyzes the hydrolysis of dienelactone to maleylacetate.⁸¹ An increase in abundance of 3-ketoacyl-(acyl-carrier-protein)-reductase (ACPR) was also detected. This enzyme is involved in type II fatty acid biosynthesis and catalyzes the reduction, by NADPH, of 3-oxoacyl-[acyl-carrier protein] to 3-hydroxyacyl-[acyl-carrier protein] (EC 1.1.1.100). The increase in these proteins involved in lipid metabolism can be related to epicuticular wax synthesis, which affects water loss occurring during cuticle transpiration.⁸²

Protein Involved in Amino Acid Metabolism. Free amino acids, particularly glutamate and aspartic acid, are essential nonvolatile compounds involved in the overall taste of many foods.⁸³ Three proteins, namely, aspartate aminotransferase (AsAT) cytoplasmic, glutamine cytosolic synthetase (GLS), and glutamine amidotransferase-like domain (GAT), involved in amino acid metabolism were found as sharply overexpressed after veraison and stably maintained at high levels during withering. This observation is in agreement with the significant transcript abundance of the cytoplasmic forms of AsAT and GLS together with asparagine synthetase observed in water-deficit-stressed mature berries.⁶² GAT coordinates the activity of two functional sites: it catalyzes the hydrolysis of glutamine at the glutaminase site and transfers the ammonia product to a synthase site only after acceptor binding, in order to avoid waste of glutamine.⁸⁴ The increase of nitrogen requirement during berry growth induces cells to transform a large amount

of glutamate via glutamine synthetase and aspartate via aspartate aminotransferase.¹⁸

GLS plays an important role in the primary assimilation of nitrogen. It catalyzes the assimilation of ammonia into glutamine and, through the glutamine synthetase-glutamate synthase cycle, is used to generate glutamate. The glutamate thus formed is the nitrogen donor for the AsAT enzyme, which uses oxalacetate and glutamate as substrates to form aspartate.⁸⁵ The aspartate is the precursor for several essential amino acids that are involved in osmotic regulation and represent the link between the nitrogen and carbon metabolic pathways. Moreover, it has been proposed in previous studies that the metabolic activity of GLS and nitrate reductase in plants is directly induced by sucrose confirming the strong correlation between N and C metabolic pathways.^{86,87} The simultaneous activation of the Krebs cycle and nitrogen metabolism we observed at proteomic level may be a result of the increase in sucrose content of the berries during the dehydration process.

Protein Associated with Cytoskeleton. In our analysis, we identified five differentially expressed protein spots related to cell structure. Four spots with different mass were identified as actin (ACT) isoforms. Similar deviations from hypothetical molecular weight of actin-assigned spots were described by Giribaldi et al.¹⁷ and could be only partially explained by degradation. Two spots with the expected mass and isoelectric point (41.7 kDa and pI 5.3 respectively) showed an evident accumulation during ripening followed by a constant expression from harvest to withering phase. This trend could reflect a cytoskeleton structure remodelling of the berry taking place after veraison, associated with the intensive cell expansion.⁸⁸ A similar trend was observed for a spot with a lower molecular weight but unmodified isoelectric point, which may be considered a cleaved product. A different pattern was observed for a high mass actin-assigned spot, which decreased after veraison. The abundance of a spot corresponding to α tubulin (TUB- α) also decreased during both ripening and withering in berry. A crucial role of TUB- α is expected during the first phase of berry development characterized by an active cell division that requires the synthesis of microtubules to drive chromosome segregation during mitosis. The rate of cell division gradually decreases during ripening being substituted by cell expansion.

Protein Associated with Synthesis, Folding and Energy-Electron Transport. The abundance of spots identified as proteasome α (Pa) and ribosomal L10 (RPL10) decreased during berry development/withering, suggesting a more active protein turnover in green tissue. A weak activation was observed during withering which may be due to a water-deficit response.²⁰ The proteasome is a multicatalytic proteinase complex able to regulate degradation of proteins into peptides.⁸⁹ RPL10 is a structural constituent of the large ribosomal subunit (60S) and is highly conserved throughout eukaryotes.⁹⁰ It is known to act as a translational regulator.⁹¹ The down regulation of Pa and RPL10 is an indirect confirmation of the generally lower protein synthesis in the mature and withered berry. Moreover, we identified one spot, namely, protein tyrosine kinase (PTK), as decreased in abundance during ripening and withering, substantiating the decrease of enzyme activity in mature and postharvest berries. The PTK is an enzyme able to transfer a phosphate group from ATP to a tyrosine residue.⁹² Phosphorylation of proteins by kinases represents an important mechanism involved in signal transduction for regulation of enzyme activity.

Members of the heat shock proteins (HSP) family, rubisco subunit binding protein (RuBP) (members of the Hsp60/GroEL family) and alpha-Crystallin-type heat shock protein (HSP) (members of 17.5 kDa Hsp) were also differentially expressed. These proteins functionally cooperate at the beginning of maturation to minimize aggregation of newly synthesized proteins facilitating the folding process.⁹³ We observed that they were highly expressed at veraison, while their abundance decreased during maturation and withering likely due to a less important role of these proteins at these stages.

The reduced role of photosynthesis in mature and withered berries is demonstrated at the proteomic level, by a decreased expression of RuBP and additionally by the low accumulation of three isoforms of the manganese-stabilizing protein/photosystem II polypeptide (MnSpPSII), involved in photosynthesis, which is also reflected in the decrease of chlorophyll pigments during ripening.

Two spots representing the mitochondrial F1-F0 ATP synthase α and β subunits (FatpA and FatpB respectively), components of the catalytic machinery involved in ATP synthesis, were identified. FatpA decreased immediately after veraison, whereas FatpB accumulated but its expression profile showed a sharp decrease after ripening, indicating that specific isoforms of mitochondrial protein are activated after veraison.

Although 2-DE is not the method of choice to detect transcription factors due to the low level of expression, a putative transcription factor (TF), which is thought to bind to the hexose transporter *VvHT1* (*Vitis vinifera* hexose transporter 1) promoter region, was identified as differentially expressed. Its expression profile showed a slight induction during ripening, and a new peak during the withering stage. In grape berries, *VvHT1* promoter is activated after induction⁹⁴ of invertases corresponding to sugar accumulation after veraison.⁹⁵

Miscellaneous. The abundance of a protein spot belonging to the cupin superfamily, classified on the basis of a conserved β -barrel fold, showed a sharp decrease after veraison. Previous studies estimated that the cupin superfamily can be divided into 18 different subclasses characterized by a remarkable chemical diversity, comprising both enzymatic and nonenzymatic members, and by a versatile protein folding.⁹⁶ Another spot, namely, DUF-642, with unknown function was found accumulate during the whole process of ripening/withering.

3.3. Transcript-Protein Comparative Analysis. As a confirmation of the active metabolism in grape berry during postharvest withering, we compared the expression profile of some significant proteins, which were shown to be activated in the proteomic analysis (chitinase, beta-1,3-glucanase, and actin), with the corresponding gene expression profile obtained from a microarray analysis of the same berry samples. The result of this parallel expression analysis over development and withering is reported in Figure 6. For the three analyzed proteins, we found an evident correspondence with the gene expression profile, particularly during the withering phase. The expression of both chitinase and glucanase transcripts during postharvesting has already been reported as a possible response to biological stress,⁹⁷ as well as actin transcript accumulation possibly linked to cellular structure remodeling occurring in withered berry.⁵

Although this analysis was limited to a few proteins whose sequences showed a certain correspondence to transcript accessions, the obtained results reinforced the observation of a metabolic activity in grape berry even after three months postharvesting.

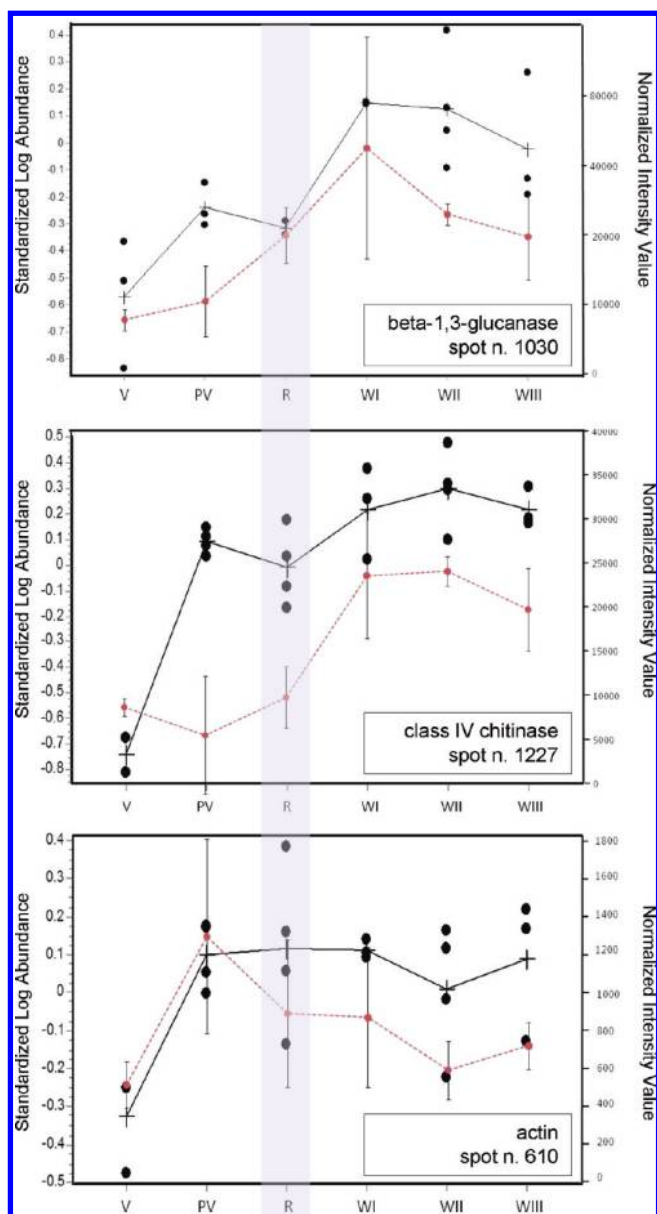


Figure 6. Comparative protein (black line) and transcript (red broken line) accumulation profiles of beta-1,3-glucanase, class IV chitinase, and actin over veraison (V), postveraison (PV), ripening (R) marked with the blue box and three stages of withering (WI, WII, WIII). Protein expression variation was expressed as average normalized volumes (left scale). Transcript variation was expressed as log₂ of mean expression value of three biological replicates, normalized for signal intensity (right scale). The number of the protein spot (related to Table 1) is reported in the boxes.

4. Conclusions

This work provides the first extensive description of grape berry proteome dynamics during the withering. As a reference variety, we chose *V. vinifera* Corvina black cultivar, which is used to produce special aroma red wine (Amarone). Proteome maps at six stages, including veraison, ripening, harvest, and withering, have been compared enabling the elucidation of metabolic pathways involved in the postharvest drying process which influences grape and wine quality.

During ripening, grape berry changes its metabolism from aerobic to anaerobic, which is reflected in the production of

ethanol, CO₂, and fermentation bioproducts. In addition, another effect of the withering process is dehydration of the berry, which results in an increase in the concentrations of sugars. The activation of stress-response proteins, the accumulation of proteins involved in flavonoid pathway, the coordinated induction of the glycolytic enzymes, and the regulation of proteins related to berry cell structure were demonstrated to be the principal responses that characterized the late ripening phase and the withering process. Moreover, some proteins, such as osmotin and enzymes involved in wax deposition, increased in abundance during withering, as a likely consequence of the dehydration stress.

We observed that many of the variations in protein abundance partially correlate with changes in their respective transcripts.^{5,7,62,70} In particular, the modifications in the principal metabolic categories during berry maturation/withering showed a similar trend at both transcriptomic and proteomic levels. Conversely, the expression profile of other proteins did not directly correspond with transcript levels, reflecting both the diverse analytic potential of the two “omic” approaches and the nonsynchronous activation of processes at different levels of biological complexity.

Our results provide evidence that an active metabolism still occurs during postharvest drying process and that many withering metabolic pathways are already activated during ripening. This substantiates the applicative value of withering as an industrial practice to confer unique and appreciable wine properties.

Abbreviations: Phe, phenol; TCA, trichloroacetic acid; ASB-14, 3-[N,N-dimethyl(3- myristoylamino)propyl]ammonio]-propanesulfonate; DTT, dithiothreitol; 2D-DIGE, two-dimensional differential in gel electrophoresis; MS, mass spectrometry.

Acknowledgment. We thank Svenja Hester and Dr. Johanna Rees for their valuable contribution during MS/MS analysis and database searches. We wish to thank also Dr. Bruno Bacher for his support with the DIGE system. This work was supported by the “BACCA” Project funded by the ORVIT Consortium, by the “Completamento del Centro di Genomica Funzionale Vegetale” Project funded by the CARIVERONA Bank Foundation, and by the “Structural and functional characterization of the grapevine genome (Vigna)” Project funded by the Italian Ministry of Agricultural and Forestry Policies (MIPAF). The authors also thank Pasqua Vini e Cantine (Verona, Italy) for allowing us to sample material from their vineyard.

Supporting Information Available: Supplemental figures and tables. This material is available free of charge via the Internet at <http://pubs.acs.org/>.

References

- (1) Deluc, L. G.; Grimplet, J.; Wheatley, M. D.; Tillett, R. L.; Quilici, D. R.; Osborne, C.; Schooley, D. A.; Schlauch, K. A.; Cushman, J. C.; Cramer, G. R. Transcriptomic and metabolite analyses of Cabernet Sauvignon grape berry development. *BMC Genomics* **2007**, *22*, 8–429.
- (2) Conde, C.; Silva, P.; Fontes, N.; Dias, A. C. P.; Tavares, R. M.; Sousa, M. J.; Agasse, A.; Delrot, S.; Geros, H. Biochemical changes throughout grape berry development and fruit and wine quality. *Food* **2007**, *1*, 1–22.
- (3) Son, H. S.; Hwang, G. S.; Kim, K. M.; Ahn, H. J.; Park, W. M.; Van Den Berg, F.; Hong, Y. S.; Lee, C. H. Metabolomic studies on geographical grapes and their wines using 1H NMR analysis coupled with multivariate statistics. *J. Agric. Food Chem.* **2009**, *57*, 1481–90.

- (4) Bellincontro, A.; De Santis, D.; Botondi, R.; Villa, I.; Mencarelli, F. Different postharvest dehydration rate affects quality characteristics and volatile compounds of Malvasia, Trebbiano and Sangiovese grapes for wine production. *J. Sci. Food Agric.* **2004**, *84*, 1791–1800.
- (5) Zamboni, A.; Minoia, L.; Ferrarini, A.; Tornielli, G. B.; Zago, E.; Delledonne, M.; Pezzotti, M. Molecular analysis of post-harvest withering in grape by AFLP transcriptional profiling. *J. Exp. Bot.* **2008**, *59*, 4145–59.
- (6) Costantini, V.; Bellincontro, A.; De Santis, D.; Botondi, R.; Mencarelli, F. Metabolic changes of Malvasia grapes for wine production during post-harvest drying. *J. Agric. Food Chem.* **2006**, *54*, 3334–3340.
- (7) Grimplet, J.; Deluc, L. G.; Tillett, R. L.; Wheatley, M. D.; Schlauch, K. A.; Cramer, G. R.; Cushman, J. C. Tissue-specific mRNA expression profiling in grape berry tissues. *BMC Genomics* **2007**, *8*, 187–210.
- (8) Wan, S. B.; Wang, W.; Wen, P. F.; Chen, J. Y.; Kong, W. F.; Pan, Q. H.; Zhan, J. C.; Tian, L.; Liu, H. T.; Huang, W. D. Cloning of phospholipase D from grape berry and its expression under heat acclimation. *J. Biochem. Mol. Biol.* **2007**, *40*, 595–603.
- (9) Wang, W.; Wan, S. B.; Zhang, P.; Wang, H. L.; Zhan, J. C.; Huang, W. D. Prokaryotic expression, polyclonal antibody preparation of the stilbene synthase gene from grape berry and its different expression in fruit development and under heat acclimation. *Plant Physiol. Biochem.* **2008**, *46*, 1085–92.
- (10) Versari, A.; Parpinello, G. P.; Tornielli, G. B.; Ferrarini, R.; Giulivo, C. Stilbene compounds and stilbene synthase expression during ripening, wilting and UV treatment in grape cv Corvine. *J. Agric. Food Chem.* **2001**, *49*, 5531–5536.
- (11) Jaillon, O.; Aury, J. M.; Noel, B.; Policriti, A.; Clepet, C.; Casagrande, A.; Choise, N.; Aubourg, S.; Vitulo, N.; Jubin, C.; Vezzi, A.; Legeai, F.; Huguency, P.; Dasilva, C.; Horner, D.; Mica, E.; Jublot, D.; Poulain, J.; Bruyère, C.; Billault, A.; Segurens, B.; Gouyvenoux, M.; Ugarte, E.; Cattonaro, F.; Anthouard, V.; Vico, V.; Del Fabbro, C.; Alaux, M.; Di Gasparo, G.; Dumas, V.; Felice, N.; Paillard, S.; Juman, I.; Moroldo, M.; Scalabrin, S.; Canaguier, A.; Le Clainche, I.; Malacrida, G.; Durand, E.; Pesole, G.; Laucou, V.; Chatelet, P.; Merdinoglu, D.; Delledonne, M.; Pezzotti, M.; Lecharny, A.; Scarpelli, C.; Artiguenave, F.; Pè, M. E.; Valle, G.; Morgante, M.; Caboche, M.; Adam-Blondon, A. F.; Weissenbach, J.; Quétiér, F.; Wincker, P. The grapevine genome sequence suggests ancestral hexaploidization in major angiosperm phyla. *Nature* **2007**, *449*, 463–7.
- (12) Grimplet, J.; Cramer, G. R.; Dickerson, J. A.; Mathiason, K.; Van Hemert, J.; Fennell, A. Y. VitisNet: “Omics” Integration through Grapevine Molecular Networks. *PLoS One* **2009**, *4*, e8365.
- (13) Velasco, R.; Zharkikh, A.; Troggio, M.; Cartwright, D. A.; Cestaro, A.; Pruss, D.; Pindo, M.; Fitzgerald, L. M.; Vezzulli, S.; Reid, J.; Malacarne, G.; Iliev, D.; Coppola, G.; Wardell, B.; Micheletti, D.; Macalma, T.; Facci, M.; Mitchell, J. T.; Perazzolli, M.; Eldredge, G.; Gatto, P.; Ozyerski, R.; Moretto, M.; Gutin, N.; Stefanini, M.; Chen, Y.; Segala, C.; Davenport, C.; Demattè, L.; Mraz, A.; Battilana, J.; Stormo, K.; Costa, F.; Tao, Q.; Si-Ammour, A.; Harkins, T.; Lackey, A.; Perbost, C.; Taillon, B.; Stella, A.; Solovyev, V.; Fawcett, J. A.; Sterck, L.; Vandepoele, K.; Grand, S. M.; Toppo, S.; Moser, C.; Lanchbury, J.; Bogden, R.; Skolnick, M.; Sgaramella, V.; Bhatnagar, S. K.; Fontana, P.; Gutin, A.; Van de Peer, Y.; Salamini, F.; Viola, R. A high quality draft consensus sequence of the genome of a heterozygous grapevine variety. *PLoS One* **2007**, *19*, e1326.
- (14) Rotter, A.; Camps, C.; Lohse, M.; Kappel, C.; Pilati, S.; Hren, M.; Stitt, M.; Coutos-Thévenot, P.; Moser, C.; Usadel, B.; Delrot, S.; Gruden, K. Gene expression profiling in susceptible interaction of grapevine with its fungal pathogen *Eutypa lata*: extending MapMan ontology for grapevine. *BMC Plant Biol.* **2009**, *5*, 9–104.
- (15) Pilati, S.; Perazzolli, M.; Malossini, A.; Cestaro, A.; Demattè, L.; Fontana, P.; Dal Ri, A.; Viola, R.; Velasco, R.; Moser, C. Genome-wide transcriptional analysis of grapevine berry ripening reveals a set of genes similarly modulated during three seasons and the occurrence of an oxidative burst at véraison. *BMC Genomics* **2007**, *8*, 428–450.
- (16) Zenoni, S.; Ferrarini, A.; Giacomelli, E.; Xumerle, L.; Fasoli, M.; Malerba, G.; Bellin, D.; Pezzotti, M.; Delledonne, M. Characterization of transcriptional complexity during berry development in *Vitis vinifera* using RNA-Seq. *Plant Physiol.* **2010**, *152*, 1787–95.
- (17) Giribaldi, M.; Perugini, I.; Sauvage, F. X.; Schubert, A. Analysis of protein changes during grape berry ripening by 2-DE and MALDI-TOF. *Proteomics* **2007**, *7*, 3154–70.
- (18) Deytieu, C.; Geny, L.; Lapaillerie, D.; Claverol, S.; Bonneau, M.; Donèche, B. Proteome analysis of grape skins during ripening. *J. Exp. Bot.* **2007**, *58*, 1851–62.
- (19) Negri, A. S.; Prinsi, B.; Rossoni, M.; Failla, O.; Scienza, A.; Cocucci, M.; Espen, L. Proteome changes in the skin of the grape cultivar Barbera among different stages of ripening. *BMC Genomics* **2008**, *8*, 9–378.
- (20) Grimplet, J.; Wheatley, M. D.; Jouira, H. B.; Deluc, L. G.; Cramer, G. R.; Cushman, J. C. Proteomic and selected metabolite analysis of grape berry tissues under well watered and water-deficit stress conditions. *Proteomics* **2009**, *9*, 2503–28.
- (21) Sarry, J. E.; Sommerer, N.; Sauvage, F. X.; Bergoin, A.; Rossignol, M.; Albagnac, G.; Romieu, C. Grape berry biochemistry revisited upon proteomic analysis of the mesocarp. *Proteomics* **2004**, *4*, 201–15.
- (22) Lund, S. T.; Bohlmann, J. The molecular basis for wine grape quality - A volatile subject. *Science* **2006**, *311*, 804–805.
- (23) Ferreira, R. B.; Piçarra-Pereira, M. A.; Monteiro, S. S.; Loureiro, V. B.; Teixeira, A. R. The wine proteins. *Trends Food Sci. Technol.* **2002**, *12*, 230–239.
- (24) Peyrot des Gachons, C.; Kennedy, J. A. Direct method for determining seed and skin proanthocyanidin extraction into red wine. *J. Agric. Food Chem.* **2003**, *51*, 5877–5881.
- (25) Peng, Z.; Hayasaka, Y.; Iland, P. G.; Sefton, M.; Høj, P.; Waters, E. J. Quantitative analysis of polymeric procyanidins (tannins) from grape *Vitis vinifera* seeds by reverse phase high-performance liquid chromatography. *J. Agric. Food Chem.* **2001**, *49*, 26–31.
- (26) Vincent, D.; Wheatley, M. D.; Cramer, G. R. Optimization of protein extraction of mature grape berry clusters. *Electrophoresis* **2006**, *27*, 1853–1865.
- (27) Coombe, B. G. Adoption of a system for identifying grapevine growth stages. *Aust. J. Grape Wine Res.* **1995**, *1*, 104–110.
- (28) Tsugita, A.; Kamo, M. 2-D electrophoresis of plant proteins. *Methods Mol. Biol.* **1999**, *112*, 95–97.
- (29) Oakley, B. R.; Kirsch, D. R.; Morris, N. R. A simplified ultrasensitive silver stain for detecting proteins in polyacrylamide gels. *Anal. Biochem.* **1980**, *105*, 361–3.
- (30) Shevchenko, A.; Wilm, M.; Vorm, O.; Mann, M. Mass Spectrometric Sequencing of Proteins from Silver-Stained Polyacrylamide Gels. *Anal. Chem.* **1996**, *68*, 850–8.
- (31) Unlü, M.; Morgan, M. E.; Minden, J. S. Difference gel electrophoresis: a single gel method for detecting changes in cell extracts. *Electrophoresis* **1999**, *18*, 2071–2077.
- (32) Di Carli, M.; Villani, M. E.; Renzone, G.; Nardi, L.; Pasquo, A.; Franconi, R.; Scaloni, A.; Benvenuto, E.; Desiderio, A. Leaf proteome analysis of transgenic plants expressing antiviral antibodies. *J. Proteome Res.* **2009**, *8*, 838–848.
- (33) Coulthurst, S. J.; Lilley, K. S.; Hedley, P. E.; Liu, H.; Toth, I. K.; Salmond, G. P. DsbA plays a critical and multi-faceted role in the production of secreted virulence factors by the phytopathogen, *Erwinia carotovora* subsp. *atroseptica*. *J. Biol. Chem.* **2008**, *283*, 23739–53.
- (34) Ashburner, M.; Ball, C. A.; Blake, J. A.; Botstein, D.; Butler, H.; Cherry, J. M.; Davis, A. P.; Dolinski, K.; Dwight, S. S.; Eppig, J. T.; Harris, M. A.; Hill, D. P.; Issel-Tarver, L.; Kasarskis, A.; Lewis, S.; Matese, J. C.; Richardson, J. E.; Ringwald, M.; Rubin, G. M.; Sherlock, G. Gene ontology: tool for the unification of biology. The Gene Ontology Consortium. *Nat. Genet.* **2000**, *25*, 25–29.
- (35) Rouillard, J. M.; Zuker, M.; Gulari, E. OligoArray 2.0: design of oligonucleotide probes for DNA microarrays using a thermodynamic approach. *Nucleic Acids Res.* **2003**, *31*, 3057–3062.
- (36) Rezaian, M. A.; Krake, L. R. Nucleic acid extraction and virus detection in grapevine. *J. Virol. Methods* **1987**, *17*, 277–285.
- (37) Smyth, G. K.; Speed, T. P. Normalization of cDNA microarray data. *Methods* **2003**, *31*, 265–273.
- (38) Brennan, T.; Frenkel, C. Involvement of hydrogen peroxide in the regulation of senescence in pear. *Plant Physiol.* **1977**, *59*, 411–416.
- (39) Jimenez, A.; Creissen, G.; Kular, B.; Firmin, J.; Robinson, S.; Verhoeven, M.; Mullineaux, P. Changes in oxidative processes and components of the antioxidant system during tomato fruit ripening. *Planta* **2002**, *214*, 751–758.
- (40) Rogiers, S. Y.; Kumar, M. G. N.; Knowles, N. R. Maturation and ripening of fruit of *Amelanchier alnifolia* Nutt. are accompanied by increasing oxidative stress. *Ann. Bot.* **1998**, *81*, 203–211.
- (41) Terrier, N.; Glissant, D.; Grimplet, J.; Barrieu, F.; Abbal, P.; Couture, C.; Georges, A.; Atanassova, R.; Léon, C.; Renaudin, J. P.; Dédal-déchamp, F.; Romieu, C.; Delrot, S.; Hamdi, S. Isogene specific oligo arrays reveal multifaceted changes in gene expression during grape berry (*Vitis vinifera* L.) development. *Planta* **2005**, *222*, 832–47.
- (42) Alfenito, M. R.; Souer, E.; Goodman, C. D.; Buell, R.; Mol, J.; Koes, R.; Walbot, V. Functional complementation of anthocyanin sequestration in the vacuole by widely divergent glutathione S-transferases. *Plant Cell.* **1998**, *10*, 1135–49.

- (43) Mayer, A. M.; Harel, E. Phenoloxidases and their Significance in Fruit and Vegetables. In *Food Enzymology*; Fox, P. F., Eds.; London: Elsevier, 1991; pp 373–398.
- (44) Frenette Charron, J. B.; Breton, G.; Badawi, M.; Sarhan, F. Molecular and structural analyses of a novel temperature stress-induced lipocalin from wheat and Arabidopsis. *FEBS Lett.* **2002**, *517*, 129–32.
- (45) Renault, A. S.; Deloire, A.; Letinois, I.; Kraeva, E.; Tesniere, C.; Ageorges, A.; Redon, C.; Bierné, J. Beta-1,3-glucanase gene expression in grapevine leaves as a response to infection with *Botrytis cinerea*. *Am. J. Enol. Vitic.* **2000**, *51*, 81–87.
- (46) Cosgrove, D. J. Expansive growth of plant cell walls. *Plant Physiol. Biochem.* **2000**, *38*, 109–24.
- (47) Waters, E. J.; Shirley, N. J.; Williams, P. J. J. Nuisance proteins of wine are grape pathogenesis-related proteins. *Agric. Food Chem.* **1996**, *44*, 3–5.
- (48) Waters, E. J.; Hayasaka, Y.; Tattersall, D. B.; Adams, K. S.; Williams, P. J. Sequence analysis of grape (*Vitis vinifera*) berry chitinases that cause haze formation in wines. *J. Agric. Food Chem.* **1998**, *46*, 4950–4957.
- (49) Robinson, S. P.; Jacobs, A. K.; Dry, I. B. A Class IV Chitinase is highly expressed in grape berries during ripening. *Plant Physiol.* **1997**, *114*, 771–8.
- (50) Derckel, J. P.; Baillieul, F.; Manteau, S.; Audran, J. C.; Haye, B.; Lambert, B.; Legendre, L. Differential induction of grapevine defenses by two strains of *Botrytis cinerea*. *Physiopathology* **1999**, *89*, 197–203.
- (51) Jacobs, A. K.; Dry, I. B.; Robinson, S. P. Induction of different pathogenesis-related cDNAs in grapevine infected with powdery mildew and treated with ethephon. *Plant Pathol.* **1999**, *48*, 325–336.
- (52) Busam, G.; Kassemeyer, H. H.; Matern, U. Differential expression of chitinases in *Vitis vinifera* L. responding to systemic acquired resistance activators or fungal challenge. *Plant Physiol.* **1997**, *115*, 1029–38.
- (53) Hayasaka, Y.; Adams, K. S.; Pocock, K. F.; Baldock, G. A.; Waters, E. J.; Høj, P. B. Use of electrospray mass spectrometry for mass determination of grape *Vitis vinifera* juice pathogenesis-related proteins: A potential tool for varietal differentiation. *J. Agric. Food Chem.* **2001**, *49*, 1830–9.
- (54) Hong, J. K.; Jung, H. W.; Lee, B. K.; Lee, S. C.; Lee, Y. K.; Hwang, B. K. *Physiol. Mol. Plant Pathol.* **2004**, *64*, 301–310.
- (55) Rodrigo, I.; Vera, P.; Tornero, P.; Hernández-Yago, J.; Conejero, V. cDNA cloning of viroid-induced tomato pathogenesis-related protein P23. Characterization as a vacuolar antifungal factor. *Plant Physiol.* **1993**, *102*, 939–45.
- (56) Stintzi, A.; Heitz, T.; Kauffmann, S.; Legrand, M.; Fritig, B. Identification of a basic pathogenesis-related, thaumatin-like protein of virus-infected tobacco as osmotin. *Physiol. Mol. Plant Pathol.* **1991**, *38*, 137–46.
- (57) Jia, Y.; Martin, G. B. Rapid transcript accumulation of pathogenesis-related genes during an incompatible interaction in bacterial speck disease-resistant tomato plants. *Plant Mol. Biol.* **1999**, *40*, 455–65.
- (58) Bryngelsson, T.; Gre'en, B. Characterization of pathogenesis-related, thaumatin-like protein isolated from barley challenger with an incompatible race of mildew. *Physiol. Mol. Plant Pathol.* **1989**, *35*, 45–52.
- (59) Grillo, S.; Leone, A.; Xu, Y.; Tucci, M.; Francione, R.; Hasegawa, P. M.; Monti, M.; Bressan, R. A. Control of osmotin gene expression by ABA and osmotic stress. *Physiol. Plant.* **1995**, *93*, 498–504.
- (60) Newton, S. S.; Duman, J. G. An osmotin-like cryoprotective protein from bittersweet nightshade *Solanum dulcamara*. *Plant Mol. Biol.* **2000**, *44*, 581–589.
- (61) Salzman, R. A.; Tikhonova, I.; Bordelon, B. P.; Hasegawa, P. M.; Bressan, R. A. Coordinate accumulation of antifungal proteins and hexoses constitutes a developmentally controlled defense response during fruit ripening in grape. *Plant Physiol.* **1998**, *117*, 465–472.
- (62) Deluc, L. G.; Quilici, D. R.; Decendit, A.; Grimplet, J.; Wheatley, M. D.; Schlauch, K. A.; Méillon, J. M.; Cushman, J. C.; Cramer, G. R. Water deficit alters differentially metabolic pathways affecting important flavor and quality traits in grape berries of Cabernet Sauvignon and Chardonnay. *BMC Genomics* **2009**, *8*, 10–212.
- (63) Hiratsuka, S.; Onodera, H.; Kawai, Y.; Kubo, T.; Itoh, H.; Wada, R. ABA and sugar effects on anthocyanin formation in grape berry cultured in vitro. *Sci. Hortic.* **2001**, *90*, 121–130.
- (64) Bray, E. A. Drought- and ABA-Induced Changes in Polypeptide and mRNA Accumulation in Tomato Leaves. *Plant Physiol.* **1988**, *88*, 1210–1214.
- (65) Davies, C.; Robinson, S. P. Sugar accumulation in grape berries. Cloning of two putative vacuolar invertase cDNAs and their expression in grapevine tissues. *Plant Physiol.* **1996**, *111*, 275–83.
- (66) Or, E.; Baybik, J.; Sadka, A.; Ogrudovitch, A. Fermentative metabolism in grape berries: Isolation and characterization of pyruvate decarboxylase cDNA and analysis of its expression throughout berry development. *Plant Sci.* **2000**, *156*, 151–158.
- (67) Speirs, J.; Lee, E.; Holt, K.; Yong-Duk, K.; Steele Scott, N.; Loveys, B.; Schuch, W. Genetic manipulation of alcohol dehydrogenase levels in ripening tomato fruit affects the balance of some flavor aldehydes and alcohols. *Plant Physiol.* **1998**, *117*, 1047–58.
- (68) Tesniere, C.; Torregrosa, L.; Pradal, M.; Souquet, J. M.; Gilles, C.; Dos Santos, K.; Chatelet, P.; Gunata, Z. Effects of genetic manipulation of alcohol dehydrogenase levels on the response to stress and the synthesis of secondary metabolites in grapevine leaves. *J. Exp. Bot.* **2006**, *57*, 91–9.
- (69) Davies, C.; Robinson, S. P. Differential screening indicates a dramatic change in mRNA profiles during grape berry ripening. Cloning and characterization of cDNAs encoding putative cell wall and stress response proteins. *Plant Physiol.* **2000**, *122*, 803–12.
- (70) Castellari, S. D.; Pfeiffer, A.; Sivilotti, P.; Degan, M.; Peterlunger, E.; Di Gasparo, G. Transcriptional regulation of anthocyanin biosynthesis in ripening fruits of grapevine under seasonal water deficit. *Plant Cell Environ.* **2007**, *30*, 1381–99.
- (71) Faria, M. A.; Beja-Pereira, M.; Martin, A.; Ferriera, M. A.; Nunes, M. E. S. Grapevine clones discriminated using stilbene synthase-chalcone synthase markers. *J. Sci. Food Agric.* **2004**, *84*, 1186–1192.
- (72) Laskowski, M. J.; Dreher, K. A.; Gehring, M. A.; Abel, S.; Gensler, A. L.; Sussex, I. M. FQR1, a novel primary auxin-response gene, encodes a flavin mononucleotide-binding quinone reductase. *Plant Physiol.* **2002**, *128*, 578–90.
- (73) Bianco, L.; Lopez, L.; Scalone, A. G.; Di Carli, M.; Desiderio, A.; Benvenuto, E.; Perrotta, G. Strawberry proteome characterization and its regulation during fruit ripening and in different genotypes. *J. Proteomics* **2009**, *72*, 586–607.
- (74) Seemann, M.; Tse Sum Bui, B.; Wolff, M.; Miginiac-Maslow, M.; Rohmer, M. Isoprenoid biosynthesis in plant chloroplasts via the MEP pathway: direct thylakoid/ferredoxin-dependent photoreduction of GcpE/IspG. *FEBS Lett.* **2006**, *580*, 1547–52.
- (75) Hoenicke, K.; Borchert, O.; Grüning, K.; Simat, T. J. Untypical aging off-flavor in wine: synthesis of potential degradation compounds of indole-3-acetic acid and kynurenine and their evaluation as precursors of 2-aminoacetophenone. *J. Agric. Food Chem.* **2002**, *50*, 4303–9.
- (76) Numan, K. J.; Davies, C.; Robinson, S. P.; Fincher, G. B. Expression patterns of cell wall-modifying enzymes during grape berry development. *Planta* **2001**, *214*, 257–264.
- (77) Cosgrove, D. J. Enzymes and other agents that enhance cell wall extensibility. *Annu. Rev. Plant Physiol. Plant Mol. Biol.* **1999**, *50*, 391–417.
- (78) Chen, F.; Nonogaki, H.; Bradford, K. J. A gibberellin-regulated xyloglucan endotransglycosylase gene is expressed in the endosperm cap during tomato seed germination. *J. Exp. Bot.* **2002**, *53*, 215–223.
- (79) Bray, E. A. Genes commonly regulated by water-deficit stress in *Arabidopsis thaliana*. *J. Exp. Bot.* **2004**, *55*, 2331–2341.
- (80) Campbell, P.; Braam, J. Xyloglucan endotransglycosylases: diversity of genes, enzymes and potential wall-modifying functions. *Trends Plant Sci.* **1999**, *4*, 361–366.
- (81) Beveridge, A. J.; Ollis, D. L. A theoretical study of substrate-induced activation of diene lactone hydrolase. *Protein Eng.* **1995**, *8*, 135–142.
- (82) Rogiers, S. Y.; Hatfield, J. M.; Jaudzems, V. G.; White, R. G.; Keller, M. Grape berry cv. Shiraz epicuticular wax and transpiration during ripening and pre-harvest weight loss. *Am. J. Enol. Vitic.* **2004**, *55*, 121–127.
- (83) Boggio, S. B.; Palatnik, J. F.; Heldt, H. W.; Valle, E. M. Changes in amino acid composition and nitrogen metabolizing enzymes in ripening fruits of *Lycopersicon esculentum* Mill. *Plant Sci.* **2000**, *159*, 125–133.
- (84) Mouilleron, S.; Golinelli-Pimpaneau, B. Conformational changes in ammonia-channeling glutamine amidotransferases. *Curr. Opin. Struct. Biol.* **2007**, *17*, 653–664.
- (85) Schiavon, M.; Ertani, A.; Nardi, S. Effects of an alfalfa protein hydrolysate on the gene expression and activity of enzymes of the tricarboxylic acid (TCA) cycle and nitrogen metabolism in *Zea mays* L. *J. Agric. Food Chem.* **2008**, *56*, 11800–11808.
- (86) Silvente, S.; Reddy, P. M.; Khandual, S.; Blanco, L.; Alvarado-Affiantranger, X.; Sanchez, F.; Lara-Flores, M. Evidence for sugar signalling in the regulation of asparagine synthetase gene ex-

- pressed in *Phaseolus vulgaris* roots and nodules. *J. Exp. Bot.* **2008**, 59, 1279–1294.
- (87) Larios, B.; Agüera, E.; Cabello, P.; Maldonado, J. M.; de la Haba, P. The rate of CO₂ assimilation controls the expression and activity of glutamine synthetase through sugar formation in sunflower (*Helianthus annuus* L) leaves. *J. Exp. Bot.* **2004**, 55, 69–75.
- (88) Thomas, P.; Schiefelbein, J. Cloning and characterization of an actin depolymerizing factor gene from grape (*Vitis vinifera* L.) expressed during rooting in stem cuttings. *Plant Sci.* **2002**, 162, 283–288.
- (89) Kurepa, J.; Smalle, J. A. Structure, function and regulation of plant proteasomes. *Biochimie* **2008**, 90, 324–335.
- (90) Dick, F. A.; Trumpower, B. L. Heterologous complementation reveals that mutant alleles of QSR1 render 60S ribosomal subunits unstable and translationally inactive. *Nucleic Acids Res.* **1998**, 26, 2442–2448.
- (91) Imai, A.; Komura, M.; Kawano, E.; Kuwashiro, Y.; Takahashi, T. A semi-dominant mutation in the ribosomal protein L10 gene suppresses the dwarf phenotype of the *acl5* mutant in *Arabidopsis thaliana*. *Plant J.* **2008**, 56, 881–890.
- (92) Bose, R.; Holbert, M. A.; Pickin, K. A.; Cole, P. A. Protein tyrosine kinase-substrate interactions. *Curr. Opin. Struct. Biol.* **2006**, 16, 668–675.
- (93) Fink, A. L. Chaperone-mediated protein folding. *Physiol. Rev.* **1999**, 79, 425–449.
- (94) Davies, C.; Boss, P. K.; Robinson, S. P. Treatment of grape berries, a nonclimacteric fruit with a synthetic auxin, retards ripening and alters the expression of developmentally regulated genes. *Plant Physiol.* **1997**, 115, 1155–1161.
- (95) Fillion, L.; Ageorges, A.; Picaud, S.; Coutos-Thévenot, P.; Lemoine, R.; Romieu, C.; Delrot, S. Cloning and expression of a hexose transporter gene expressed during the ripening of grape berry. *Plant Physiol.* **1999**, 120, 1083–1094.
- (96) Dunwell, J. M.; Purvis, A.; Khuri, S. Cupins: the most functionally diverse protein superfamily. *Phytochemistry* **2004**, 65, 7–17.
- (97) Romero, I.; Sanchez-Ballesta, M. T.; Maldonado, R.; Escribano, M. I.; Merodio, C. Expression of class I chitinase and β -1,3-glucanase genes and postharvest fungal decay control of table grapes by high CO₂ pretreatment. *Postharvest Biol. Technol.* **2006**, 41, 9–15.

PR1005313